2018-02

The Evolution of the Silver Hills Volcanic Center, and Revised 40Ar/39Ar Geochronology of Montserrat, Lesser Antilles, With Implications for Island Arc Volcanism

Hatter, SJ

10.1002/2017GC007053
Geochemistry, Geophysics, Geosystems
American Geophysical Union

DOI 10.1002/2017GC007053

The evolution of the Silver Hills volcanic center, and revised $^{40}Ar/^{39}Ar$ geochronology of Montserrat, Lesser Antilles, with implications for island arc volcanism

S. J. Hatter[1], M. R. Palmer[1], T. M. Gernon[1], R. N. Taylor[1], P. D. Cole[2], D. N. Barfod[3], and M. Coussens[1]

[1]School of Ocean and Earth Science, National Oceanography Centre, University of Southampton, European Way, Southampton SO14 3ZH, UK.

[2]School of Geography, Earth and Environmental Sciences, Plymouth University, Drake Circus, Plymouth PL4 8AA, UK.

[3]Scottish Universities Environmental Research Centre, Rankine Avenue, Scottish Enterprise Park, East Kilbride G75 0QF, UK.

Corresponding author: Stuart Hatter (sjh1e13@soton.ac.uk)

Key points:

- Silver Hills volcanism was dominated by andesite dome growth and collapse, Vulcanian style eruptions and periodic sector collapse
- New ages reveal overlap in volcanic activity between the Silver and Centre Hills, and Centre and Soufriere Hills
- An older, previously unreported stage of Soufrière Hills activity at ~450–290 ka erupted hornblende-orthopyroxene lavas

Received: Jun 06, 2017; Revised: Nov 02, 2017; Accepted: Jan 20, 2018

Abstract

Studying the older volcanic centers on Montserrat, Centre Hills and Silver Hills, may reveal how volcanic activity can change over long time periods (≥1 Myr), and whether the recent activity at the Soufrière Hills is typical of volcanism throughout Montserrat's history. Here, we present the first detailed mapping of the Silver Hills, the oldest and arguably least studied volcanic center on Montserrat. Volcanism at the Silver Hills was dominated by episodic andesite lava dome growth and collapse, produced Vulcanian style eruptions, and experienced periodic sector collapse events, similar to the style of volcanic activity that has been documented for the Centre Hills and Soufrière Hills. We also present an updated geochronology of volcanism on Montserrat, by revising existing ages and obtaining new $^{40}Ar/^{39}Ar$ dates and palaeomagnetic ages from marine tephra layers. We show that the centers of the Silver, Centre, and Soufrière Hills were active during at least ~2.17–1.03 Ma, ~1.14–0.38 Ma, and ~0.45 Ma–present, respectively. Combined with timings of volcanism on Basse-Terre, Guadeloupe these ages suggest that ~0.5–1 Ma is a common lifespan for volcanic centers in the Lesser Antilles. These new dates identify a previously unrecognized overlap in activity between the different volcanic centers, which appears to be a common phenomenon in island arcs. We also identify an older stage of Soufrière Hills activity ~450–290 ka characterized by the eruption of hornblende-orthopyroxene-phyric lavas, demonstrating that the petrology of the Soufrière Hills eruptive products has changed at least twice throughout the volcano's development.

1. Introduction

Lava dome growth and collapse is a common process at arc volcanoes, e.g. as observed at Merapi volcano, Indonesia (Andreastuti et al., 2000), Mt St Helens, USA (Hoblitt et al., 1980) and Unzen volcano, Japan (Hoshizumi et al., 1999), but volcanic activity can be highly variable over the lifetime of an individual volcanic edifice (e.g. Hildreth & Lanphere, 1994; Komorowski et al., 2005; Myers et al., 1985; Pioli et al., 2015). This is exemplified in the Lesser Antilles arc, where volcanism is dominated by dome-forming eruptions, but varies in composition and style both between discrete volcanic edifices on individual islands, and during the lifetime of an individual volcano. For example, eruptive activity at volcanic centers on Guadeloupe and Martinique has varied from effusive basaltic lava flows forming shield volcanoes, to andesitic dome eruptions to Plinian eruptions (Germa et al., 2011a, 2011b; Komorowski et al., 2005; Maury et al., 1990; Samper et al., 2007). Understanding what causes these changes in eruption styles is crucial to aiding predictions concerning the long-term behavior of a volcano.

Volcanism on Montserrat has been of particular interest since the onset of renewed volcanism at the Soufrière Hills Volcano in 1995. As a consequence, it has become one of the most studied volcanoes on Earth. Since 1995 the eruption has had substantial social and economic impacts on the island, including destroying its capital, Plymouth (Kokelaar, 2002), and so gaining insight into the evolution of volcanic activity at Soufrière Hills through time is of considerable interest. Both marine and terrestrial records show that the style of past Soufrière Hills activity has changed little throughout its known ca. 282 kyr history (e.g. Le Friant et al., 2008; Smith et al., 2007), but it may not necessarily continue to behave in this way. For example, Caricchi et al. (2014) suggest that larger eruptions tend to occur towards the end of a volcano's lifetime, raising the possibility that future Soufrière Hills eruptions may be of higher magnitude. Within this context, it is important to note that Soufrière Hills is the latest in a series of volcanic centers on Montserrat. Thus, study of the extinct volcanoes on Montserrat provides an opportunity to

investigate volcanic activity over longer time periods, on the order of ~1 Myr, in order to document possible changes. Here, we provide the first detailed account of the physical volcanology of Montserrat's oldest volcanic center, the Silver Hills, in an attempt to better understand how its activity has evolved through time. We also present supporting data and observations from a marine sediment core that contains eruption products from Montserrat, and provide new $^{40}Ar/^{39}Ar$ dates for the Silver, Centre and Soufrière Hills to better constrain the timing of volcanic activity, providing an updated chronology of volcanism on the island.

2. Geological Setting

Montserrat is an active volcanic island in the Lesser Antilles Arc (Figure 1a), formed from the westward subduction of Atlantic crust beneath the Caribbean plate at a rate of *ca.* 2 cm yr^{-1} (Minster & Jordan, 1978). Detailed geological mapping of Montserrat was first carried out by Macgregor (1938), who identified seven discrete volcanoes, based on the island's geomorphology. This was revised by Rea (1974), who used K-Ar dates to identify six volcanoes, with different relative ages to those proposed by Macgregor (1938). The K-Ar dates of Rea (1974) indicate that activity on Montserrat began at ~4.3 Ma at Roche's Bluff. However, more recent $^{40}Ar/^{39}Ar$ dating by Harford et al. (2002) suggests that Montserrat is comprised of only three volcanic centers: Silver Hills (*ca*. 2580–1160 ka), Centre Hills (*ca*. 1021–550 ka) and South Soufrière Hills-Soufrière Hills (*ca*. 282 ka to present; Figure 1b). Of these centers, the Silver Hills is the least studied. It is a deeply eroded volcanic center consisting of two-pyroxene andesite (Rea, 1974) with volcaniclastic sequences, debris avalanche deposits and areas of extensive hydrothermal alteration (Harford et al., 2002). The Centre Hills consists of two-pyroxene andesite and hornblende-hypersthene andesite (Rea, 1974) with block-and-ash flow, pumice-and-ash flow, pumice-fall, lahar, fluvial and debris avalanche deposits (Harford et al., 2002). The deposits of the Centre Hills also provide evidence for the largest known eruptions on Montserrat, up to magnitude 5 (Coussens et al., 2017).

The earliest identified period of activity at the Soufrière Hills volcanic center began ~280 ka with the eruption of two-pyroxene andesites up until ~130 ka. At ~130 ka a period of mafic volcanism formed the South Soufrière Hills (Harford et al., 2002), with deposits dominated by basaltic to basaltic andesite lava flows with mass-wasting and scoria-fall deposits, and some andesitic fallout (Cassidy et al., 2014; Harford et al., 2002; Rea, 1974). Andesites erupted from Soufrière Hills following ~130 ka exhibit a different mineralogy, changing from two-pyroxene andesites to hypersthene-hornblende andesites (Harford et al., 2002). The largest known eruptions of Soufrière Hills occurred during Episode 2, ~174 ka (Coussens et al., 2017; Harford et al., 2002; Smith et al., 2007). This period of activity produced multiple pumice-rich pyroclastic density current deposits 1–3 m thick and a pumice fall deposit 1 m thick ~3 km from the probable source, providing the only evidence of possible Plinian eruptions from the Soufrière Hills volcano.

Currently, the Soufrière Hills comprises a central dome complex surrounded by volcaniclastic deposits, which are andesitic in composition. The dome complex comprises four old domes: Chances Peak (<200 ka), Gages Mountain (151 ± 8 ka), Galway's Mountain (112 ± 18 ka) and Perches Mountain (24 ± 4 ka) (Harford et al., 2002), and a dome within English's Crater created by the recent eruption (1995–2010; Figure 1b). The modern dome covers a fifth older dome, Castle Peak (formed *ca*. 1650 AD) (Young et al., 1996), and has undergone multiple successive growth and collapse phases during the recent eruption. Indeed, the current eruptive phase has been dominated by a combination of Vulcanian explosions, dome growth and dome collapse

events (Kokelaar, 2002; Wadge et al., 2014), which is probably characteristic of Soufrière Hills activity over the past ~280 kyr (Rea, 1974; Roobol & Smith, 1998; Smith et al., 2007).

Large landslide deposits discovered offshore of Montserrat reveal that Soufrière Hills has undergone multiple flank collapse events (Coussens et al., 2016; Deplus et al., 2001; Le Friant et al., 2004; Lebas et al., 2011). Additionally, a debris avalanche occurred during the recent eruption on 26th December 1997, resulting from dome growth over a hydrothermally weakened sector of the wall of English's crater (Sparks et al., 2002; Voight et al., 2002).

3. Methods

3.1. Field Work

Field mapping was undertaken in the Silver Hills, Montserrat in May 2014 and 2015 at a scale of 1:25000, with samples collected for $^{40}Ar/^{39}Ar$ dating and geochemical analysis. The Silver Hills is highly eroded with a current subaerial area of ~6.5 km^2. The patchy nature of exposures coupled with the generally limited spatial extent of individual units means that radiometric dates are vital to constrain a stratigraphy for the Silver Hills deposits.

3.2. $^{40}Ar/^{39}Ar$ Dating

Twelve lava and three pumice samples were prepared at the Scottish Universities Environmental Research Centre (SUERC) Argon Isotope Facility (AIF), where they were crushed in a jaw-crusher, sieved in to a 250–500 μm size fraction, leached in 20% HNO_3, and passed through a Frantz magnetic barrier laboratory separator (model LB-1) to separate plagioclase phenocrysts from the groundmass. Plagioclase separates were then leached in 5% HF to remove any glass attached to the crystals. 200 mg and 1 g of clean plagioclase phenocryst separates and groundmass (lavas only), respectively, were then hand-picked for $^{40}Ar/^{39}Ar$ dating.

The samples were irradiated for one hour in the Oregon State University reactor, Cd-shielded facility, and analyzed on a GVi instruments ARGUS V multi-collector mass spectrometer using a variable sensitivity faraday collector array in static collection (non-peak hopping) mode (Mark et al., 2009; Sparks et al., 2008) at SUERC AIF. Alder Creek sanidine (1.2056 ± 0.0019 Ma, 1σ) (Renne et al., 2011) was used to monitor ^{39}Ar production and establish neutron flux values (J) for the samples. The reader is directed to Coussens et al. (2017) for more details of the method. The average total system blank for laser extractions, measured between each sample run, was $1.5 \pm 0.7 \times 10^{-15}$ mol ^{40}Ar, $1.2 \pm 1.3 \times 10^{-17}$ mol ^{39}Ar and $8.5 \pm 3.6 \times 10^{-18}$ mol ^{36}Ar for lava samples, and $1.7 \pm 0.1 \times 10^{-15}$ mol ^{40}Ar, $1.6 \pm 0.5 \times 1.1^{-17}$ mol ^{39}Ar and $1.6 \pm 0.7 \times 10^{-17}$ mol ^{36}Ar for pumice samples. All blank, interference and mass discrimination calculations were performed with the *MassSpec* software package (versions 8.058 and 8.16 for andesite and pumice samples respectively, authored by Al Deino, Berkeley Geochronology Center).

Plateau ages, or composite plateau ages for replicated samples, are chosen as the best estimates of the emplacement ages. Accepted plateau ages must be derived from a minimum of three contiguous steps (minimum ^{39}Ar content of each step is ≥0.1% of total ^{39}Ar release) which overlap in age within 2σ uncertainty, and contains a minimum of 50% of ^{39}Ar released for the combined steps. The scatter between ages of the steps must be low with a MSWD (mean square weighted deviation) less than the 95% probability cut-off (Wendt & Carl, 1991). Further, the inverse isochron formed by the plateau steps must yield an age indistinguishable from the plateau age at 2σ uncertainty, and the $^{40}Ar/^{36}Ar$ of the trapped component composition derived from the

inverse isochron must be indistinguishable from the composition of air (298.56 ± 0.61, 2σ) at the 2σ uncertainty level.

For fall deposits or ignimbrites, the single crystal approach is used to determine an eruptive age because this allows for discrimination of juvenile crystals and crystals derived from other sources, e.g., xenocrysts or antecrysts, but pumice samples yielded low-K plagioclase that could not be analyzed as single crystals. Instead, a multi-grain, two-step heating approach was adopted to increase signal sizes allowing for more precise measurements. The presence of older xenocrysts in these multi-grain aliquots could bias age results, an effect dependent on the age of the xenocryst and its relative potassium content. To account for this possibility, the experiment was repeated (n≥15) and the youngest, Gaussian distributed population of ages was calculated from the set of analyses.

Each individual gas analysis represents an aliquot of 50-100 single grains, loaded into a 4 mm well in a copper planchette. An initial step at ~0.5 watts of power was used to drive off atmospheric gas and liberate argon from any alteration phases that might be present. A second fusion step at 15 watts of power yielded age information associated with the plagioclase crystals.

3.3. Whole Rock Geochemistry

Nb and Y were analyzed on a VG Plasmaquad PQ2+ ICP-MS multi-element analyzer at the University of Southampton following the method of Coussens et al. (2017), in which 0.05 g of powdered sample is analyzed. Precision is better than 3%.

Pb and Nd isotopes were measured from 50 and 200 mg (for pumice and lava samples respectively) of hand-picked rock chips 0.5–1 mm in size. Samples were leached and digested following the method of Cassidy et al. (2012), and Pb was isolated from the matrix using AGX-1x8 200-400 mesh anion exchange resin, following the method of Kamber and Gladu (2009). For Nd, the dissolved samples were first passed through cation columns containing AG50-X8 200-400 mesh resin, then through LN Spec columns (Eichrom Industries, Illinois, USA). Pb and Nd isotopes were measured on a MC-ICP-MS (Neptune) at the University of Southampton. Pb isotopes were corrected for instrumental mass fractionation using the SBL74 double spike (Taylor et al., 2015). SRM NBS981 gave $^{206}Pb/^{204}Pb = 16.9400 \pm 0.0023$, $^{207}Pb/^{204}Pb = 15.4965 \pm 0.0026$ and $^{208}Pb/^{204}Pb = 36.7124 \pm 0.0076$ on n = 108 measurements during the course of this study. Measured values for standard JNdi are $^{143}Nd/^{144}Nd = 0.512116 \pm 0.000012$ (n = 36).

3.4. Core Sample Acquisition

Samples were analyzed from marine sediment core U1396C, from International Ocean Discovery Program (IODP) Expedition 340. This site is located ~35 km southwest of Montserrat (Figure 1a). The core is 145.92 m long and provides a record extending back ~4.5 Ma (Expedition 340 scientists, 2013). This study investigates the tephra layers deposited in the past ~2.35 Ma (the interval represented by the terrestrial record on Montserrat), which have been sampled for geochemical analysis. These samples have been previously analyzed for Pb isotopes by Palmer et al. (2016).

4. Timing of Montserrat Volcanism

4.1. Existing $^{40}Ar/^{39}Ar$ Dates

The $^{40}Ar/^{39}Ar$ ages of Montserrat from previous studies are compiled in Table 1. All of these studies used the same strict criteria outlined above (section 3.2) to determine plateau ages. The

ages of Harford et al. (2002) and Brown and Davidson (2008) have been recalculated with modern decay constants and standard ages using the Renne et al. (2010, 2011) optimization model, resulting in slightly increased ages. All ages referenced from these authors are the recalculated ages (see supporting information Table S1 for original and recalculated ages). Here, we review the dates from these previous studies to identify which ages are reliable, and which should be viewed with caution.

Harford et al. (2002) obtained ages for all of the Montserrat volcanic centers (Figure 1b; Table 1). Some of their ages, however, should be viewed with caution, as either their plateau profiles contain evidence of xenocrystic components or Ar recoil, they have a saddle-shaped plateau typical of lavas with excess argon, or have a MSWD which exceeds the critical 95% confidence level. Of the dates considered reliable, two are from the Centre Hills, six are from the Soufrière Hills, and three are from the South Soufrière Hills, with none from the Silver Hills (Table 1).

Five $^{40}Ar/^{39}Ar$ ages were acquired for the Silver Hills by Brown and Davidson (2008), in the range of ~1.52–1.40 Ma, but only cover a small area of the Silver Hills center, four of which are part of the same stratigraphic sequence (Figure 2; Table 1). These ages were measured from groundmass (i.e. no xenocrystic material). Coussens et al. (2017) obtained five $^{40}Ar/^{39}Ar$ ages from Centre Hills deposits (~0.79–0.48 Ma; Figure 1b; Table 1) and one from a fault block within the Centre Hills (~1.31 Ma), which they interpret as originating from the Silver Hills volcanic center. These ages were obtained from plagioclase phenocrysts, so the presence of xenocrysts cannot be ruled out.

The questionable quality of the Silver Hills ages reported by Harford et al. (2002), and the limited spatial and stratigraphic extent of the Silver Hills ages reported in Brown and Davidson (2008) mean that the timing of volcanic activity is poorly known for the Silver Hills. This highlights the need for new $^{40}Ar/^{39}Ar$ dates, to better constrain the timing of Silver Hills activity, and aid the development of a detailed stratigraphy of the Silver Hills deposits.

4.2. New $^{40}Ar/^{39}Ar$ Dates

Here we present fifteen new $^{40}Ar/^{39}Ar$ ages for Montserrat (Figures 3–4; Table 2; supporting information Tables S2–3): geographically eleven are from the Silver Hills (~2.17–0.45 Ma; Figure 2) and four are from the Centre Hills (~1.04–0.38 Ma; Figure 1b). All samples produced plateau ages that match our strict criteria. The first run of sample 17/76-AL did not yield a plateau, however, and therefore did not meet the criteria for a reliable age, whereas the second run yielded a release profile that meets our criteria and yielded an age of 1.18 ± 0.30 Ma. Nevertheless, this age is viewed with caution as overall the sample shows significant heterogeneity and non-reproducible release spectra (Figure 3).

Harford et al. (2002) note evidence for xenocrysts in their ages obtained from plagioclase phenocrysts, leading them to interpret these ages as maximum ages, rather than true eruption ages. The influence of xenocrysts in our sample ages can be assessed by examining the data from samples 05/03-AL and 15/70-AC, for which both groundmass and plagioclase ages were measured. For both samples the plagioclase age is systematically older than the groundmass age, suggesting that the plagioclase may contain a minor xenocrystic component, but there is overlap in the 2σ errors of the two phases, which suggests that the plagioclase ages encompass the true eruption age within their 2σ errors. The plagioclase ages obtained by Coussens et al. (2017) also likely represent the eruption ages, because they were obtained on similar material, and have similar scale 2σ errors.

In the following sections, only the dates that are considered to be reliable are used in developing a detailed stratigraphy of the Silver Hills deposits, and when discussing the timing of volcanic activity.

5. Lithofacies of the Silver Hills Deposits

Here we adopt the non-genetic terminology of volcanic rocks proposed by White and Houghton (2006); lithofacies terms and abbreviations used are given in Table 3. For debris avalanche deposits we use the terms "megablock facies" (Voight et al., 2002) and "matrix facies" (Crandell et al., 1984; Voight et al., 2002).

5.1. Lava and Intensely Hydrothermally Altered Lava

The lava exposures are dominantly composed of plagioclase-pyroxene-phyric andesite (~30–60 vol. % phenocrysts), with minor dacite and basaltic andesite with the same phenocryst populations. Lava thickness ranges from meters to hundreds of meters, with some exposures showing alignment of elongate crystals. The lava commonly locally transitions to breccia.

In some regions the lava flows are extensively hydrothermally altered to an extent that no primary magmatic minerals are identifiable, and they exhibit a crumbly texture. The present day exposures may be white or orange and yellow in color, with the latter being associated with abundant centimeter-scale gypsum crystals. These altered exposures are surrounded by a halo of less hydrothermally altered rocks, with the degree of hydrothermal alteration decreasing outward.

5.1.1. Interpretation

The lavas form lava flows and domes, and the transitioning to breccia is interpreted as resulting from local autobrecciation of the lava along its margins. The zones of intensely hydrothermally altered lava are interpreted as the sites of fumarolic activity on the Silver Hills. The presence of gypsum crystals and pervasive variable discoloration make them comparable to the recent deposits of Galway's Soufrière (Voight et al., 2002), which also shows the intensity of hydrothermal alteration decreasing with distance from the fumaroles.

5.2. Massive to Diffusely Stratified, Lapilli-Tuff to Tuff-Breccia (m-dsLT-TBr)

The m-dsLT-TBr are poorly sorted, variably clast- and matrix-supported and consist of centimeter- to meter-scale sub-rounded to angular andesite clasts, up to 20% of which are hydrothermally altered. Some units of this facies display normal and inverse grading at their upper and lower boundaries, respectively.

5.2.1. Interpretation

This facies is interpreted as block-and-ash flow deposits due to its massive structure, poor sorting, clast size range and grading. These characteristics are comparable to the block-and-ash flow deposits produced by dome collapses at Soufrière Hills Volcano during the 1995–2010 eruption (Cole et al., 2002; Stinton et al., 2014).

5.3. Massive Tuff-Breccia and Breccia, with Megablocks (mTBr-Br_{MB})

This facies is similar in appearance to the m-dsLT-TBr facies, but with three key differences: absence of grading, presence of jigsaw-fit fractures in some clasts, and the occurrence of megablocks. The megablocks are tens to hundreds of meters in scale, and can be split into two categories: lava megablocks and volcaniclastic megablocks. Lava megablocks vary from poorly-

to highly-fractured and show variable hydrothermal alteration. Some of the megablocks are faulted. Volcaniclastic megablocks are blocks of other volcaniclastic facies (e.g. mLT) hosted within surrounding mTBr, and are either composed of a single unit or a layered sequence. Some megablocks are sheared, and others contain parts which appear to intrude into the surrounding breccia. Interdigitation of units within layered volcaniclastic megablocks is common. Most boundaries between megablocks and breccia are sharp, but some display signs of mixing.

5.3.1. Interpretation

The presence of megablocks within the mTBr suggests that they are parts of debris avalanche deposits; the megablocks are large coherent fragments of the original volcanic edifice that have been transported by debris avalanches with little internal deformation. Layered volcaniclastic megablocks may preserve their original structure and stratigraphy. The matrix facies consists of a poorly-sorted massive breccia formed from the mingling of disaggregated megablocks and entrained material. Jigsaw-fit fracturing of clasts is a common feature of debris avalanche deposits (e.g. Crandell et al., 1984; Ui, 1983; Ui & Glicken, 1986), as are the fluidal textures at the edges of megablocks and deformation of units within individual volcaniclastic megablocks (e.g. interdigitation of units) (e.g. Takarada et al., 1999; Ui & Glicken, 1986; van Wyk de Vries & Davies, 2015). Faulting is another well-documented feature of some megablocks (e.g. Glicken, 1996; Ui et al., 1986; Ui & Glicken, 1986; van Wyk de Vries & Davies, 2015).

5.4. Massive Lapilli-Tuff, with regular Lapilli-Tuff and Tuff-Breccia Lenses (mLTlensLT-TBr)

The mLT are poorly-sorted, matrix-supported and consist of centimeter-scale rounded to sub-rounded andesite clasts, ~10% of which are hydrothermally altered. The LT-TBr lenses are poorly sorted, clast supported and consist of centimeter- to decimeter-scale rounded andesite clasts, up to 5% of which are hydrothermally altered. They typically have meter- and decimeter-scale length and thickness, respectively, with decimeter-scale spacing.

5.4.1. Interpretation

This facies is interpreted as lahar deposits, on the basis that they contain multiple coarse lenses of rounded to sub-rounded andesite clasts in variably massive and parallel to cross-stratified coarse ash to coarse lapilli. They are similar to modern lahar deposits present in the Belham Valley, on the west flank of Soufrière Hills (Barclay et al., 2007).

5.5. Pumiceous, Massive to Diffusely Stratified, Lapilli-Tuff to Tuff-Breccia (pm-dsLT-TBr)

This facies can be split into two subfacies: well-sorted and poorly-sorted. Occurrences of the well-sorted subfacies are clast-supported with centimeter-scale sub-angular to angular clasts of andesitic pumice and andesite. Clast proportions are typically ~90% pumice and ~10% andesite, with the pumice clasts being consistently coarser than the andesite clasts. Exposures of the poorly-sorted subfacies are variably clast- and matrix-supported and consist of centimeter- to decimeter-scale rounded to angular clasts. The clast proportions are typically in the range of 65–99% pumice, 1–33% andesite and 0–5% HA andesite. Locally, exposures of this subfacies have erosional bases.

5.5.1. Interpretation

The well-sorted subfacies are interpreted as primary fallout deposits, due to the high degree of sorting and predominance of angular pumice with subordinate smaller lithics. The poorly-sorted subfacies are interpreted as pumice-and-ash flow deposits, due to their poor sorting, rounded clasts and erosional bases, similar to pumice-and-ash flow deposits produced from recent Vulcanian eruptions of Soufrière Hills (Cole et al., 2002, 2014).

6. Stratigraphy of the Silver Hills

6.1. Little Bay to South Drummonds, >2 Ma

The oldest dated unit is an isolated exposure of dacitic mLT-TBr at south Drummonds. This unit contains meter-scale blocks, has a minimum thickness of 3 m, and is dated at 2.170 ± 0.180 Ma (Figure 2).

6.2. Marguerita Ghaut and North Marguerita Bay, ~1.7–1.6 Ma

Marguerita Ghaut contains mTBr and coherent andesite and basaltic andesite lava exposures, with sharp boundaries between them. The mTBr has an age of 1.682 ± 0.094 Ma (Figure 2). The eastern mouth of the ghaut contains a ~35 m thick sequence of mTBr, and an andesite block from the base of this sequence has an age of 1.634 ± 0.083 Ma (Figure. 2). North Marguerita Bay contains a debris avalanche deposit consisting of a volcaniclastic megablock overlain by a $mTBr_{MB}$ (Figure 5; see supporting information Text S1 for a detailed description).

6.3. Yellow Hole to Old Quaw, ~1.5 Ma

The Yellow Hole exposures consist of extensively hydrothermally altered andesite lava overlain by non-altered lava dated at 1.520 ± 0.051 Ma (Brown & Davidson, 2008). At the mouth of Old Quaw ghaut is a debris avalanche deposit (Figure 2), with a megablock of hydrothermally altered lava next to non-altered mBr (matrix facies), and the boundary between them varies from sharp to transitional. There is an isolated block of the breccia within the hydrothermally altered lava, most likely resulting from internal deformation during transport (Siebert, 1984).

6.4. North West Bluff, ~1.5–4 Ma

North West Bluff is a ~200 m high peak made of andesite lava with areas of local (<1 m^2) hydrothermal alteration, and an age of 1.493 ± 0.098 Ma. Exposure of this lava continues as a ridge heading southeast from North West Bluff to Valentine Hill (Figure 2), which consists of hydrothermally altered lava overlain by non-altered lava. In northwest Thatch Valley, the lavas have undergone extensive hydrothermal alteration, and locally becomes the 'intensely hydrothermally altered lava' facies.

North-central Thatch Valley contains a ~45 m thick (minimum) mTBr which has an age of 1.450 ± 0.160 Ma (Figure 2). Some clasts contain jigsaw-fit fractures, which supports an origin as a debris avalanche deposit, but the limited size of the exposure, coupled with the buried boundaries with surrounding units makes this difficult to confirm.

The andesite and dacite lava around and north of Rendezvous Bay is of a similar age, 1.424 ± 0.080 Ma (Figure 2). There is exposure of 'intensely hydrothermally altered lava' midway between Rendezvous Bay and North West Bluff.

6.5. Silver Hill, ~1.4 Ma

Andesite lavas and mLT-Br's tens of meters thick are exposed alongside the road between Drummonds and Silver Hill, and have been dated at 1.430 ± 0.019 to 1.395 ± 0.017 Ma (Brown

& Davidson, 2008) (Figure 2). Rendezvous Bluff consists of a ~50 m high sequence of m-dsTBr overlying the lavas of Rendezvous Bay. Near Rendezvous they have a flow direction away from Silver Hill (Figure 2), and so are likely contemporaneous with the block-and-ash flow deposits between Silver Hill and Drummonds.

Further block-and-ash flow deposits from this period can be found overlying the basal hydrothermally altered lava of Valentine Hill (Figure 2). A ridge of this lava extends southeast from Valentine Hill, and on the southwestern side of this ridge the lava is overlain by a ~20 m of m-dsTBr's (units V1–4) infilling a palaeovalley (Figure S1).

The lavas of Thatch Valley are locally overlain by mTBr, which locally has a hydrothermally altered matrix. These breccias are likely contemporaneous with the other mTBr units.

6.6. South Marguerita Bay, ~1.3 Ma

South Marguerita Bay contains a sequence of dacitic mLT-TBr tens of meters thick. The upper unit of this sequence is dated at 1.330 ± 0.190 Ma (Figure 2). Coussens et al. (2017) obtained an age of 1.310 ± 0.200 for their 'South Lime Kiln Bay pumice' unit, which is a poorly-sorted pmLT located in a fault block within the Centre Hills (Figure 1b). Due to its age, and location in a fault block, they interpret this deposit as originating from the Silver Hills.

6.7. Little Bay, ~1.0–0.8 Ma

The largest debris avalanche deposit of the Silver Hills is located in the Little Bay region, spanning Potato Hill, Davy Hill and Little Bay (Figure 2, S2 and S3). It consists of lava- and volcaniclastic-megablocks, with surrounding matrix facies (see supporting information Text S2 for a detailed description). Lava from a megablock east of Potato Hill has an age of 1.430 ± 0.120 Ma.

6.8. Potato Hill, ~0.8 Ma

Overlying unit PH1 at Potato Hill is a pumiceous pyroclastic sequence (units PH2–4; Figure 2 and 6a). Unit PH3 (primary fallout deposit) has been dated at 0.800 ± 0.120 Ma (Figure 2), and has a Centre Hills origin (see section 8.1). This constrains the timing of the Little Bay debris avalanche to >0.8 Ma.

6.9. Old Quaw Ghaut, ~0.45 Ma

The Old Quaw debris avalanche deposit is overlain by a horizontally bedded volcaniclastic sequence containing four units, three of which are separated by palaeosols (units OQ1–4; Figure 6b), and were likely deposited in a palaeovalley. The base of this sequence, a $mLT_{lensLT\text{-}TBr}$ (unit OQ1), is overlain by pumiceous deposits which display noticeable variation between two exposures ~60 m apart (log sites 2–3; Figures 2 and 6b). Units OQ2a and 3a laterally transition between the well- and poorly-sorted subfacies' of pmLT-TBr with small (centimeter-scale) erosional channels. At log site 2 they grade into coarser and finer grained poorly-sorted pmLT-TBr's, respectively, with higher proportions of lithic clasts and matrix. This grading of unit OQ2a is also displayed at log site 3, but here unit OQ3a is missing. Unit OQ2a has been dated at 0.450 ± 0.130 Ma. The transition between the well- and poorly-sorted subfacies within the same unit suggests that units OQ2–3 are reworked fallout deposits. This interpretation is supported by the $^{40}Ar/^{39}Ar$ age and Pb isotope data, because the pumice clasts from unit OQ2a have a Soufrière Hills signature (see section 8.1). It is considered unfeasible for a pyroclastic density current to reach the eastern Silver Hills from the Soufrière Hills, hence these pumice clasts are

likely to be derived from fallout from an eruption column. This unit is the oldest known deposit from a Soufrière Hills eruption.

7. Expanded Stratigraphy of the Centre Hills

7.1. East Coast, ~1 Ma

Sample 21/81-AC comes from a basaltic andesite mTBr on the east coast of Centre Hills (Figure 1b), which lies at the base of the stratigraphy of Coussens et al. (2017). The age of 1.040 ± 0.250 Ma is within error of the oldest dates for this center (Coussens et al., 2017; Harford et al., 2002).

7.2. Southwest Centre Hills, ~0.45 Ma

Pumice from a pumiceous mTBr in the southwest Centre Hills has an $^{40}Ar/^{39}Ar$ age of 450 ± 170 ka (Figure 1b), and a Soufrière Hills Pb isotope signature (see section 8.1). This provides further evidence for Soufrière Hills volcanism at ~450 ka.

7.3. Dry Waterfall and Spring Ghaut, ~0.38 Ma

Andesite lava from Dry Waterfall (central Centre Hills) has been dated at 378 ± 18 ka (Figure 1b), and has a Centre Hills Pb isotope value (section 8.1), providing the youngest known age for Centre Hills volcanism. A dacitic mTBr from Spring Ghaut (southwest Centre Hills) has been dated at 376 ± 85 ka (Figure 1b), and has a Soufrière Hills Pb isotope signature. This demonstrates an overlap in activity between Centre Hills and Soufrière Hills volcanism.

8. Provenance

Many intra-oceanic arcs display along-arc geochemical heterogeneity, caused by variations in source component contributions (e.g. Izu-Bonin-Mariana arc: Elliott et al. (1997); Ishizuka et al. (2007); Tonga-Kermadec-Lau arc: Ewart et al. (1998); Lesser Antilles arc: Macdonald et al. (2000)). Such variation has also been observed on individual islands, allowing the eruption deposits of distinct volcanic centers to be distinguished using isotope and trace element ratios. For example, Pagan island in the Mariana arc contains two volcanic centers ~8 km apart, Mount Pagan and South Pagan, whose eruption deposits can be distinguished using trace element ratios (e.g. Ba/Th, Ba/La, Nb/Zr) (Marske et al., 2011). The island of Hachijojima in the Izu-Bonin arc comprises two volcanic centers ~7 km apart, Higashiyama and Nishiyama, the deposits of which can be distinguished using Pb isotopes, and Zr/Y and La/Sm ratios (Ishizuka et al., 2008). In the Lesser Antilles, there is a clear north-south gradient in the Sr, Nd and Pb isotope ratios, and trace element patterns of volcanic rocks along the entire arc that has persisted for ~5 Myr (Labanieh et al., 2010; Lindsay et al., 2005). This geographical pattern is also observed on individual islands, such as Martinique, where $^{143}Nd/^{144}Nd$ can be used to separate deposits from Pitons du Carbet and Mont Conil-Mont Pelée, which overlapped in activity 545–322 ka (Germa et al., 2011b; Labanieh et al., 2012). For Montserrat, Pb isotopes have been shown to clearly distinguish Soufrière Hills deposits from those of the Centre and Silver Hills, and $^{143}Nd/^{144}Nd$ can be used to differentiate between Silver Hills and Centre Hills deposits (Cassidy et al., 2012).

For some samples in this study there is ambiguity over which volcanic center they are from, such as 16/72-PR, which is geographically within the Silver Hills, but has a Centre/Soufrière Hills age. Here, we use trace element and isotope geochemistry to help constrain their provenance (data is presented in supporting information Table S4).

8.1. Terrestrial Deposits

Most of the samples analyzed in this paper fit within the Silver Hills-Centre Hills Pb isotope field, with three samples falling in the Soufrière Hills field: 28/57-AC, 16/72-PR and 20/79-PC (Figure **7**).

Silver Hills and Centre Hills samples can be distinguished on a plot of $^{143}Nd/^{144}Nd$ vs Nb/Y (Figure 8). Four samples with uncertain origin (i.e. from either Silver Hills or Centre Hills volcanism) are highlighted on Figure 8a: pumice from Davy Hill, Potato Hill and Lime Kiln Bay, and a lava clast from South Marguerita Bay. Pumice from a fault block in South Lime Kiln Bay (sample 11.1.4C), which is geographically part of the Centre Hills, has been dated at ~1.31 Ma, leading to the interpretation that this deposit originated from Silver Hills volcanism (Coussens et al., 2017). This interpretation is supported by $^{143}Nd/^{144}Nd$ vs Nb/Y, in which this same sample plots within the Silver Hills field (Figure 8a).

The Silver Hills-Centre Hills boundary defined by Harford et al. (2002) follows Brimm's Ghaut, which runs through Marguerita Bay (Figure 2). Sample 12/13-AC from south Marguerita Bay (south of the boundary) has been dated at ~1.33 Ma, suggesting a Silver Hills origin. This is supported by $^{143}Nd/^{144}Nd$ vs Nb/Y (Figure 8a), suggesting that the boundary between the Silver Hills and Centre Hills is further south than previously thought.

Sample 23/86-PF (unit PH3 on Potato Hill) is geographically within the Silver Hills, but has an age of ~0.8 Ma, suggesting this deposit is derived from the Centre Hills (Figure 2). This interpretation is supported by a Centre Hills geochemical signature (Figure 8a). The pumice sample from Davy Hill (24/88-PC) is also geographically within the Silver Hills, but falls in the Centre Hills field in Figure 8a, suggesting a Centre Hills origin. Because this sample is part of the Little Bay debris avalanche deposit, this suggests that the debris avalanche occurred during the early stages of Centre Hills volcanism.

8.2. Marine Tephra Deposits

Marine sediment core U1396C contains fifteen tephra layers with thicknesses >1 cm within the ~2.35–0.37 Ma time span covered by our new $^{40}Ar/^{39}Ar$ ages. The age assignments of the tephra layers are derived from palaeomagnetic, biostratigraphic and foraminifera $\delta^{18}O$ correlations (Fraass et al., 2016; Hatfield, 2015). Pb isotope analyses show that thirteen of these layers are from Montserrat and the other two are from Guadeloupe (Palmer et al., 2016). Of the Montserrat layers, eight contain enough pumice or fresh non-vesicular lava grains for geochemical analysis (Table 4). Of particular interest are the five tephra layers in the 1–1.3 Ma period (the gap in the terrestrial age record between the Silver and Centre Hills) with sufficient pumice. Figure 8b shows that the layers with ages of 1.10 Ma and 1.03 Ma fall within the Silver Hills field, and 1.14, 1.08 and 1.04 Ma fall within the Centre Hills field (Figure 8b). The absolute uncertainty in the age of any individual tephra layer is ~50 kyr, but the stratigraphic order of the layers is certain. Hence, we can be confident that there was overlap in activity between the Silver and Centre Hills for at least ~130 ka.

9. Petrology

The lavas of the Silver Hills volcanic center are porphyritic (~30–60 vol. % phenocrysts) with a phenocryst assemblage of ~65–75% plagioclase up to 4 mm, ~15–20% orthopyroxene up to 6 mm and ~5–15% clinopyroxene up to 5 mm. Quartz and amphibole are locally present in minor amounts. Zoning is observed in some clinopyroxene and orthopyroxene phenocrysts, and all

plagioclase phenocrysts, with many of the latter displaying sieve textures. The groundmass is generally microcrystalline and composed of plagioclase, orthopyroxene, clinopyroxene and Fe-Ti oxides (Figure 9), with some samples showing alignment of elongate crystals.

Enclaves are abundant within Silver Hills lavas, and comprise up to 20 vol. %. They have coarser groundmasses (composed of plagioclase, orthopyroxene, clinopyroxene and Fe-Ti oxides) than the host andesite, with a higher proportion of pyroxenes (Figure 9). Many of the enclaves have a diktytaxitic groundmass, with interlocking, randomly-orientated elongate crystals, similar to enclaves erupted during the 1995–2010 eruption of the Soufrière Hills (Plail et al., 2014).

The Centre Hills samples have a similar phenocryst assemblage as the Silver Hills lavas, closely matching the samples described by Coussens et al. (2017). The Soufrière Hills samples are porphyritic (~30 vol. % phenocrysts) with a phenocryst assemblage of ~65–75% plagioclase, 15–20% orthopyroxene and 10–15% amphibole, with minor clinopyroxene and quartz, similar to the Soufrière Hills lavas erupted in the past ~130 kyr (Harford et al., 2002).

10. Discussion

10.1. Evolution of the Silver Hills Volcanic Center

Subaerial volcanic activity began in the Silver Hills prior to 2 Ma, with the oldest rocks present as lava domes around the Little Bay area and dome collapse deposits built up the south Drummonds region (Figure 10). At ~1.7–1.6 Ma, activity migrated to the eastern part of Silver Hills, forming the lava domes and associated deposits of Marguerita Bay. Part of this edifice collapsed to form the Marguerita Bay debris avalanche deposit. Activity continued in this region up until ~1.5 Ma, forming the lavas of Yellow Hole, with collapse of this edifice forming the Old Quaw debris avalanche. Next, activity shifted to the northwestern part of the Silver Hills, forming the lava domes of North West Bluff, Thatch Valley and Rendezvous Bay at ~1.5–1.4 Ma, with concomitant hydrothermal activity producing the observed fumarole deposits in this region. At ~1.4 Ma activity shifted again to form lava domes at Silver Hill and Drummonds, which collapsed to form block-and-ash flow deposits throughout the north, west and center of the Silver Hills. Collapse of these edifices with part of the young Centre Hills edifice created the Little Bay debris avalanche deposit at around ~1–0.8 Ma. The block-and-ash flow deposits of south Marguerita Bay suggest that lava dome growth was still active in the Drummonds area ~1.35–1.30 Ma (Figure 10). The youngest deposits found in the Silver Hills region are reworked pumice fall deposits in Old Quaw, which Pb isotopes indicate to be derived from eruptions of the early stages of Soufrière Hills volcanism ~0.45 Ma.

10.2. Comparisons with Soufrière Hills and Centre Hills

The Silver Hills is the smallest volcanic center on Montserrat in terms of subaerial exposure, but bathymetric data may provide an insight into its original size. Montserrat is surrounded by a shallow submarine shelf, which extends up to 5 km wide around the Silver Hills (Figure 1b), and is interpreted as representing the original expanse of the Silver Hills (Le Friant et al., 2004). Assuming that the Silver Hills originally had a similar size to the Soufrière Hills, the estimated minimum original volume of the Silver Hills above 100 m below sea level (the depth of the submarine shelf) is 17 km^3; the subaerial part of the Soufrière Hills is ~12 km^3 (Le Friant et al., 2004).

Our work on the deposits of the Silver Hills volcano has shown its past volcanic activity to be similar to that of the Soufrière Hills, with both characterized by lava dome growth and collapse coupled with Vulcanian eruptions and periodic flank/sector collapses. Soufrière Hills does, however, exhibit evidence of larger, sustained eruptions at ~450 and ~179 ka, whereas there is no record of large eruptions emanating from the Silver Hills. The Centre Hills activity is also characterized by lava dome growth and collapse with Vulcanian eruptions, but also produced multiple Plinian eruptions (possibly up to magnitude 5) throughout its eruptive history (Coussens et al., 2017; Harford et al., 2002). The consistency in the style of volcanic activity throughout the lifespan of the Silver Hills adds support to the hypothesis of Harford et al. (2002) that future activity at Soufrière Hills is likely to continue in the same style as the 1995–2010 eruption.

It is worth noting, however, that the exposed massifs of the Soufrière Hills and Centre Hills are both currently larger in size than Silver Hills, and that the Plinian deposits of both the former are situated along coastal exposures that are now missing from Silver Hills. Additionally, the current size of the sub-aerial portion of Silver Hills is approximately the same size as the central dome complex of the Soufrière Hills which, like the central part of Centre Hills, is dominated by massive andesite dome-lava and their collapse deposits (Harford et al., 2002). Thus it is feasible that any large sustained explosive eruptions that Silver Hills may have produced are not preserved on land, akin to the Basal Complex, the oldest volcanic center on Basse-Terre, Guadeloupe. This is another deeply eroded volcano whose sub-aerial record is dominated by effusive eruption products, with no evidence of large explosive activity. However, the study of a marine sediment core has revealed that this seemingly effusive center produced a large Plinian eruption (Volcanic Explosivity Index ~6) towards the end of its life, at ~2.4 Ma, which is believed to be the largest known eruption in the Lesser Antilles (Palmer et al., 2016). While the Silver Hills may not have produced eruptions of this magnitude, this example serves to highlight a potential preservation bias within the Silver Hills' terrestrial record.

10.3. Comparisons with Other Arc Volcanic Centers

Many arc volcanoes dominated by andesitic and dacitic lava dome formation nevertheless also experience periodic Plinian eruptions, similar to that inferred for the Centre Hills (Coussens et al., 2017). For example, the 1902 Plinian eruption of Santa Maria, a dominantly andesitic (Rose, 1972) stratovolcano in Guatemala, was one of the 10 largest eruptions ever observed (Bennett et al., 1992), yet volcanic activity at Santa Maria has been dominated by eruptions of lava flows and domes, with their associated collapse pyroclastic deposits (Rose, 1972, 1973, 1987). Indeed, the active Santiaguito dome complex has built up inside the crater produced from the 1902 eruption. In Chile, Volcán Quizapu produced two of the largest historic eruptions of South America, which were of a similar composition, yet one was effusive (a ~5 km^3 mingled andesite-dacite lava flow in 1846–1847), and one was explosive (a ~4.5 km^3 dacitic Plinian eruption in 1932) (Hildreth & Drake, 1992). The transition between effusive and explosive eruptions at Volcán Quizapu has been linked to the extent of mafic magma recharge and mixing prior to eruption. The 1932 Plinian eruption had a relatively minor recharge component, while the recharge magma comprised <10–45 vol% of the lava erupted throughout 1846–1847 (Ruprecht & Bachmann, 2010). The resident magma temperatures for both eruptions is estimated to be ~870°C (Ridolfi et al., 2010), but the greater volume of recharge magma of the 1846–1847 eruption led to an eruption temperature up to 130°C hotter than the 1932 eruption. It is thought that this higher magmatic temperature enhanced syneruptive magma degassing and led

to effusive eruptive behavior, by accelerating volatile diffusion, lowering melt viscosity, and inhibiting brittle fragmentation (Ruprecht & Bachmann, 2010).

Magma recharge and mixing is also considered to be responsible for the long-term (~500–0 ka) low explosivity of Mount Hood, Oregon, another andesite-dacite arc volcano with no evidence for large explosive eruptions (Koleszar et al., 2012; Scott et al., 1997). Viscosity models show that mafic recharge beneath Mount Hood may result in a 5–10-fold decrease in viscosity of the silicic resident magma, facilitating greater volatile diffusion, and delaying or precluding fragmentation during magma ascent. The continued low explosivity of activity at Mount Hood over 500 kyr is thought to be due to somewhat constant mixing proportions and timescales, whereas variability in mixing proportions and timescales leads to variation in eruption styles between effusive and explosive (Koleszar et al., 2012), such as observed at Volcán Quizapu (Ruprecht & Bachmann, 2010). Further, Koleszar et al. (2012) invoke this model to explain the long-term low explosivity (i.e. absence of Plinian eruptions) in other andesitic-dacitic arc volcanoes where magma mixing is a common process, such as Unzen volcano, Japan (Hoshizumi et al., 1999; Venezky & Rutherford, 1999), and Mount Dutton, Alaska (Miller et al., 1999).

On Montserrat, this model may also explain the low explosivity behavior of the Silver Hills and Soufrière Hills, because the lavas of these centers contain abundant mafic enclaves, indicating magma mixing has consistently played a major role in controlling eruption styles at these volcanic centers (e.g. Murphy et al., 1998; this study). Furthermore, for the Centre Hills deposits, enclaves are only present within lavas, and not in the pumiceous (explosive) deposits (Coussens et al., 2017). This suggests that the absence of, or at least reduced extent of, magma recharge and mixing may have played a significant role in producing large explosive eruptions at the Centre Hills. However, this model relies on the recharge magma raising the temperature of the resident magma to prevent explosive eruptions, but geothermometry studies estimate that magma storage temperatures beneath the Centre Hills (~810–1080°C; Coussens et al., 2017) were similar to those of the 1995–2010 Soufrière Hills eruption (~785–1100°C; Barclay et al., 1998; Christopher et al., 2014; Devine et al., 1998, 2003, Murphy et al., 1998, 2000). This suggests that increased temperature alone cannot be responsible for the explosive eruptions of the Centre Hills. Coussens et al. (2017) showed that the composition of Center Hills deposits remained constant, thus ruling out compositional control on eruption styles. They suggest instead that explosive eruptions may have been the result of local changes in magma storage conditions (variable magma temperature or viscosity) and pre-eruptive dynamics.

In the Lesser Antilles, Silver Hills volcanism is typical of that documented along the northern arc, in that andesitic dome growth and collapse—with small explosive eruptions—has dominated volcanic activity at Saba, St. Eustatius, St. Kitts, and Nevis, with no evidence for larger, sustained eruptions (Baker, 1984, 1985; Baker et al., 1980; Davidson & Wilson, 2011; Defant et al., 2001). Petrological evidence (e.g. reverse-zoned phenocrysts) indicate that magma recharge and mixing is a common process at Saba and St. Kitts (Baker et al., 1980; Toothill et al., 2007), which following the model of Koleszar et al. (2012), suggests that the characteristics of magma recharge and mixing have been constant for the northern islands, thus inhibiting the potential for large explosive eruptions and maintaining low explosivity behavior. The central and southern islands display similar activity to the northern islands, but with Plinian eruptions identified at La Soufriere, Guadeloupe (Komorowski et al., 2005), Morne Diablotins and Morne Trois Pitons-Microtrin, Dominica (Boudon et al., 2017), Mont Pelée, Martinique (Roobol & Smith, 1976;

Westercamp & Traineau, 1983), Qualibou, St Lucia (Wohletz et al., 1986), and Soufrière, St Vincent (Rowley, 1978; Wright et al., 1984), more akin to the Centre Hills volcanism (Coussens et al., 2017). In Dominica, mafic enclaves are present in lavas from multiple volcanic centers, but are notably absent from pumiceous deposits (Howe et al., 2015), further supporting a link between magma recharge and mixing and eruption explosivity. Further detailed studies comparing evidence for magma mixing (e.g. enclave abundances, reverse-zoned phenocrysts) between eruption styles are required to further investigate the link between magma mixing and eruption explosivity in the Lesser Antilles.

10.4. Revised Geochronology of Volcanism on Montserrat

Here, we present a revised geochronology of volcanic activity of Montserrat's three main volcanic centers (Figure 11), based on a review of existing ages, new $^{40}Ar/^{39}Ar$ dates, and palaeomagnetic ages from marine tephra layers.

Previously, Silver Hills volcanism was dated to range from ~2.6–1.2 Ma (Brown & Davidson, 2008; Harford et al., 2002), but as discussed some of these dates are unreliable. Silver Hill volcanism can now be reliably constrained to at least ~2.17–1.03 Ma. Coussens et al. (2017) divided Centre Hills volcanism into two periods of activity, spanning >0.95 to ~0.60 Ma and ~0.60 to ~0.40 Ma. The new Centre Hills dates presented in this study expand the timing of Centre Hills volcanism by ~0.2 Myr, to ~1.14–0.38 Ma.

Three stages of Soufrière Hills volcanism have been previously recognized: >300–175 ka, 175–130 ka and 112 ka to recent (Coussens et al., 2017; Harford et al., 2002). Our new ages identify a fourth, earlier stage, ~450–300 ka, characterized by the eruption of hornblende-orthopyroxene andesites, similar to lavas erupted since ~112 ka, and in contrast to the two-pyroxene andesites erupted ~290–130 ka (Harford et al., 2002; Rea, 1974). This means that the petrology of the Soufrière Hills eruptive products has changed at least twice throughout the volcano's development. Garibaldi Hill, which contains a two-pyroxene andesite block-and-ash flow deposit dated at 290 ka (Harford et al., 2002), contains both two-pyroxene and hornblende-hypersthene andesites, but the stratigraphic relationship between the two andesite types is not documented (Rea, 1974). A detailed stratigraphy of Garibaldi Hill may provide further details as to when the change from hornblende-hypersthene to two-pyroxene andesite took place, and if it was an instant or a gradual change.

Our new ages show that Silver, Centre and Soufriere Hills were active for at least 1.14 Myr, 0.76 Myr, and 0.45 Myr, respectively. The most comparable island to Montserrat in the Lesser Antilles arc is the neighboring island of Basse-Terre, Guadeloupe. It also formed following tectonic adjustments during the Mid-Miocene and similarly shows a north-south migration in the locus of volcanism over a similar time interval. There is also high quality age data available for the volcanic centers on Basse-Terre; with 2.79–2.68 Ma, 1.81–1.15 Ma, 1.02–0.44 Ma, 0.56–0.47 Ma and 0.21 Ma – present recorded for the Basal Complex, Septentrional Chain, Axial Chain, Monts Caraïbes Massif and Grande Découverte Volcanic Complex, respectively (Carlut et al., 2000; Ricci et al., 2015a, 2015b, Samper et al., 2007, 2009). With the exception of the oldest Basal Complex (which is heavily eroded and has limited subaerial exposure) and Monts Caraïbes Massif (which has limited subaerial exposure and only two dates), these intervals of activity (0.66 Myr, 0.58 Myr, and 0.21 Myr) for the different centers on Basse-Terre are similar to those observed on Montserrat. These observations suggest that ~0.5–1.0 Ma is a common lifespan for volcanic centers in the region. The question arises, therefore, as to whether this

apparent timescale of volcanic center duration is purely stochastic or whether it has more fundamental significance. For example, the duration of a volcanic center may be related to the life cycle of volcanic edifices. Modeling of edifice loading indicates that progressive growth of a volcanic structure results in the confining pressure increasing to the extent that the center is forced to migrate laterally (Pinel et al., 2010). Alternatively, the duration of a volcanic center may be related to deeper processes. For example, it has been suggested that partial melting in the mantle wedge yields rising diapirs of partially molten material that rise through the mantle with frequencies of order 10^5–10^6 years (Hall & Kincaid, 2001; Stern, 2002). Further detailed geochronology of volcanic centers on other islands of the Lesser Antilles is required to assess these hypotheses in more detail.

Our new ages also provide evidence for a ~130 kyr overlap in activity between the Silver and Centre Hills, and ~70 kyr overlap between the Centre and Soufrière Hills. There was also overlap between the Soufrière and South Soufrière Hills (Cassidy et al., 2012, 2014). Overlap in volcanic activity between two or more centers on an individual island has also been documented on Martinique, where Trois Ilets and Pitons du Carbet were both active from 998 to 345 ka. Here, further coeval activity occurred at Mont Conil-Mont Pelée during 545–345 ka (Germa et al., 2010, 2011b). On Dominica, there has been coeval activity between at least up to four volcanic centers over much of the lifetime of the island (Smith et al., 2013, and references therein). The volcanic centers of Basse-Terre, Guadeloupe have been extensively dated, and overlap in activity has only been identified between two centers: the Axial Chain and Monts Caraïbes during 555–472 ka (Carlut et al., 2000; Ricci et al., 2015a, 2015b, Samper et al., 2007, 2009).

The overlap in volcanic activity between centers on these four islands suggests that it is a common phenomenon in the Lesser Antilles and, indeed, in other arc systems. For example, in the Izu-Bonin-Mariana arc, most islands contain a single volcanic center, but islands with multiple centers have experienced coeval activity at two neighboring volcanic centers. These are: Hachijojima, where Higashiyama and Nishiyama (7 km apart) have been concurrently active for at least 10 ka (Ishizuka et al., 2008); Pagan island, where Mount Pagan and South Pagan (~8 km apart) have experienced coeval activity for at least 64 ka (Marske et al., 2011); and Izu-Oshima, which has been simultaneously active with the neighboring Izu-Tobu volcanic field for at least 40–50 ka, which at their closest are only ~4 km apart (Ishizuka et al., 2015 and references therein). The distance separating sites of coeval activity in the Izu-Bonin-Mariana and Lesser Antilles arcs (typically <10 km) relative to the depth to the melt generation zone above the subducting slab (of the order ~100 km; Stern, 2002) suggests that a rising diapir or plume of partial melt may bifurcate to form separate magma chambers at intermediate depths (~15 km; Odbert et al., 2014) beneath the individual volcanic centers.

11. Conclusions

We describe the rocks of the Silver Hills volcanic center, which are dominated by andesite lavas and breccias, formed from effusive lava dome eruptions and dome collapses. Pumiceous flow deposits are also present, providing evidence of explosive activity from Vulcanian style eruptions. There is evidence of widespread hydrothermal alteration, with three fumarole deposits identified, resulting from hydrothermal activity concurrent with Silver Hills volcanism. Four debris avalanche deposits were also identified, indicating that the volcano experienced periodic sector collapses. These observations suggest that the Silver Hills was characterized by the same type of volcanic activity as has been observed at the Centre Hills and Soufrière Hills. The

notable absence of evidence of sustained explosive eruptions at Silver Hills, which occurred in the early stages of Soufrière Hills' development and throughout Centre Hills' activity, may be the result of consistent mafic magma recharge and mixing, which could raise magma temperatures and inhibit the potential for large explosive eruptions.

New $^{40}Ar/^{39}Ar$ dates, combined with ages from marine tephra layers and a review of existing ages, have yielded a revised geochronology of volcanic activity of Montserrat's three main centers, which were active during at least ~2.17–1.03 Ma, ~1.14–0.38 Ma, and ~0.45 Ma–present for the Silver, Centre, and Soufrière Hills centers, respectively. Two key findings come from these new dates: the previously unknown overlaps in volcanic activity between both the Silver and Centre Hills and Centre and Soufrière Hills, and the discovery of a new, older stage of Soufrière Hills activity ~450–290 ka with the eruption of hornblende-orthopyroxene lavas. Combined with ages of volcanic centers on Basse-Terre, Guadeloupe, our ages suggest that ~0.5–1 Ma is a common lifespan for volcanic centers in the Lesser Antilles. Furthermore, overlap in activity between closely spaced (<10 km) volcanic centers appears to be a common phenomenon in island arcs, as it has been observed on multiple islands in the Lesser Antilles and Izu-Bonin-Mariana arcs.

12. Acknowledgments

We thank Adam Stinton and Rod Stewart for support during fieldwork, Agnes Michalik, Andy Milton and Matt Cooper for assistance with geochemical analyses, and Jim Imlach for support with $^{40}Ar/^{39}Ar$ sample preparation. We also thank Jack Palmer and Josh Brown for assistance with hand picking samples for $^{40}Ar/^{39}Ar$ dating. Brian Jicha and an anonymous reviewer are thanked for their comments, which helped improve this manuscript. $^{40}Ar/^{39}Ar$ dates were funded by NERC Isotope Geosciences Facility allocation IP-1537-0515. We also acknowledge funding from NERC IODP Case studentship NE/K007386/1. Supporting information has been provided in Text S1–2, Figures S1–3, and Tables S1–4.

13. References

Andreastuti, S. D., Alloway, B. V., & Smith, I. E. M. (2000). A detailed tephrostratigraphic framework at Merapi Volcano, Central Java, Indonesia: implications for eruption predictions and hazard assessment. *Journal of Volcanology and Geothermal Research, 100*, 51–67. doi:10.1016/S0377-0273(00)00133-5

Baker, P. E. (1985). Volcanic hazards on St Kitts and Montserrat, West Indies. *Journal of the Geological Society of London, 142*, 279–295. doi:10.1130/MEM164-p169

Baker, P. E. (1984). Geochemical evolution of St Kitts and Montserrat, Lesser Antilles. *Journal of the Geological Society of London, 141*, 401–411. doi:10.1144/gsjgs.141.3.0401

Baker, P. E., Buckley, F., & Padfield, T. (1980). Petrology of the volcanic rocks of Saba, West Indies. *Bulletin of Volcanology, 43*, 337–346. doi:10.1007/BF02598037

Barclay, J., Alexander, J., & Sušnik, J. (2007). Rainfall-induced lahars in the Belham Valley, Montserrat, West Indies. *Journal of the Geological Society of London, 164*, 815–827. doi:10.1144/0016-76492006-078

Barclay, J., Rutherford, M. J., Carroll, M. R., Murphy, M. D., Devine, J. D., Gardner, J., & Sparks, R. S. J. (1998). Experimental phase equilibria constraints on pre-eruptive storage conditions of the Soufrière Hills magma. *Geophysical Research Letters, 25*, 3437–3440.

doi:10.1029/98GL00856

Bennett, E. H. S., Rose, W. I., & Conway, F. M. (1992). Santa María, Guatemala: A decade volcano. *Eos, Transactions American Geophysical Union, 73*, 521–522. doi:10.1029/91EO00387

Boudon, G., Balcone-Boissard, H., Solaro, C., & Martel, C. (2017). Revised chronostratigraphy of recurrent ignimbritic eruptions in Dominica (Lesser Antilles arc): Implications on the behavior of the magma plumbing system. *Journal of Volcanology and Geothermal Research, 343*, 135–154. doi:10.1016/j.jvolgeores.2017.06.022

Brown, K., & Davidson, C. (2008). $^{40}Ar/^{39}Ar$ geochronology of the Silver Hills andesite, Montserrat, West Indies, (Bachelor of Arts Senior Integrative Exercise). Carlton College, Northfield, Minnesota.

Caricchi, L., Annen, C., Blundy, J., Simpson, G., & Pinel, V. (2014). Frequency and magnitude of volcanic eruptions controlled by magma injection and buoyancy. *Nature Geoscience, 7*, 126–130. doi:10.1038/ngeo2041

Carlut, J., Quidelleur, X., Courtillot, V., & Boudon, G. (2000). Paleomagnetic directions and K/Ar dating of 0 to 1 Ma lava flows from La Guadeloupe Island: Implications for time-averaged field models. *Journal of Geophysical Research, 105*, 835–849. doi:10.1029/1999JB900238

Cassidy, M., Taylor, R. N., Palmer, M. R., Cooper, R. J., Stenlake, C., & Trofimovs, J. (2012). Tracking the magmatic evolution of island arc volcanism: Insights from a high-precision Pb isotope record of Montserrat, Lesser Antilles. *Geochemistry, Geophysics, Geosystems, 13*, 1–19. doi:10.1029/2012GC004064

Cassidy, M., Trofimovs, J., Watt, S. F. L., Palmer, M. R., Taylor, R. N., Gernon, T. M., … Le Friant, A. (2014). Multi-stage collapse events in the South Soufrière Hills, Montserrat as recorded in marine sediment cores. In Wadge, G., Robertson, R. E. A., & Voight, B. (Eds.), *The eruption of the Soufrière Hills volcano, Montserrat from 2000 to 2010* (Vol. 39, pp. 383–397) London: Geological Society Memoirs. doi:10.1144/M39.20

Christopher, T. E., Humphreys, M. C. S., Barclay, J., Genareau, K., De Angelis, S. M. H., Plail, M., & Donovan, A. (2014). Petrological and geochemical variation during the Soufrière Hills eruption, 1995 to 2010. In Wadge, G., Robertson, R. E. A., & Voight, B. (Eds.), *The eruption of the Soufrière Hills volcano, Montserrat from 2000 to 2010* (Vol. 39, pp. 317–342) London: Geological Society Memoirs. doi:10.1144/M39.17

Cole, P. D., Calder, E. S., Sparks, R. S. J., Clarke, A. B., Druitt, T. H., Young, S. R., … Norton, G. E. (2002). Deposits from dome-collapse and fountain-collapse pyroclastic flows at Soufrière Hills Volcano, Montserrat. In Druitt, T. H., & Kokelaar, B. P. (Eds.), *The eruption of the Soufrière Hills volcano, Montserrat from 1995 to 1999* (Vol. 21, pp. 231–262) London: Geological Society Memoirs. doi:10.1144/GSL.MEM.2002.021.01.11

Cole, P. D., Smith, P. J., Stinton, A. J., Odbert, H. M., Bernstein, M. L., Komorowski, J. C., & Stewart, R. (2014). Vulcanian explosions at Soufrière Hills Volcano, Montserrat between 2008 and 2010. In Wadge, G., Robertson, R. E. A., & Voight, B. (Eds.), *The eruption of the Soufrière Hills volcano, Montserrat from 2000 to 2010* (Vol. 39, pp. 93–111) London: Geological Society Memoirs. doi:10.1144/M39.5

Coussens, M., Cassidy, M., Watt, S. F. L., Jutzeler, M., Talling, P. J., Barfod, D., … Palmer, M. R. (2017). Long-term changes in explosive and effusive behaviour at andesitic arc volcanoes: Chronostratigraphy of the Centre Hills Volcano, Montserrat. *Journal of Volcanology and Geothermal Research, 333–334*, 15–35. doi:10.1016/j.jvolgeores.2017.01.003

Coussens, M., Wall-Palmer, D., Talling, P. J., Watt, S. F. L., Cassidy, M., Jutzeler, … M., Stinton, A. J. (2016). The relationship between eruptive activity, flank collapse, and sea level at volcanic islands: A long-term (>1 Ma) record offshore Montserrat, Lesser Antilles. *Geochemistry, Geophysics, Geosystems, 17*, 2591–2611. doi:doi:10.1002/2015GC006053.

Crandell, D. R., Miller, C. D., Glicken, H. X., Christiansen, R. L., & Newhall, C. G. (1984). Catastrophic debris avalanche from ancestral Mount Shasta volcano, California. *Geology, 12*, 143–146. doi:10.1130/0091-7613(1984)12<143:CDAFAM>2.0.CO;2

Davidson, J., & Wilson, M. (2011). Differentiation and source processes at Mt Pelée and the Quill; Active volcanoes in the Lesser Antilles arc. *Journal of Petrology, 52*, 1493–1531. doi:10.1093/petrology/egq095

Defant, M. J., Sherman, S., Maury, R. C., Bellon, H., De Boer, J., Davidson, J., & Kepezhinskas, P. (2001). The geology, petrology, and petrogenesis of Saba Island, Lesser Antilles. *Journal of Volcanology and Geothermal Research, 107*, 87–111. doi:10.1016/S0377-0273(00)00268-7

Deplus, C., Friant, A. Le, Boudon, G., Komorowski, J. C., Villemant, B., Harford, C., … Cheminee, J. L. (2001). Submarine evidence for large-scale debris avalanches in the Lesser Antilles arc. *Earth and Planetary Science Letters, 192*, 145–157. doi:10.1016/S0012-821X(01)00444-7

Devine, J. D., Murphy, M. D., Rutherford, M. J., Barclay, J., Sparks, R. S. J., Carroll, M. R., … Gardner, J. E. (1998). Petrologic evidence for pre-eruptive pressure-temperature conditions, and recent reheating, of andesitic magma erupting at the Soufrière Hills Volcano, Montserrat, W.I. *Geophysical Research Letters, 25*, 3669–3672. doi:10.1029/98GL01330

Devine, J. D., Rutherford, M. J., Norton, G. E., & Young, S. R. (2003). Magma Storage Region Processes Inferred from Geochemistry of Fe–Ti Oxides in Andesitic Magma, Soufrière Hills Volcano, Montserrat, W.I. *Journal of Petrology, 44*, 1375–1400. doi:10.1093/petrology/44.8.1375

Elliott, T., Plank, T., Zindler, A., White, W., & Bourdon, B. (1997). Element transport from slab to volcanic front at the Mariana arc. *Journal of Geophysical Research, 102*, 14991–15019. doi: 10.1029/97JB00788

Ewart, A., Collerson, K. D., Regelous, M., Wendt, J. I., & Niu, Y. (1998). Geochemical Evolution within the Tonga-Kermadec-Lau arc-back-arc systems: the role of varying mantle wedge composition in space and time. *Journal of Petrology*, *39*, 331–368. doi:10.1093/petroj/39.3.331

Expedition 340 scientists. (2013). Site U1396. In Le Friant, A., Ishizuka, O., Stroncik, N. A., & Expedition 340 scientists. (Eds.), *Proceedings of the Integrated Ocean Drilling Program*, (Vol. 340). Tokyo: Integrated Ocean Drilling Program Management International, Inc. doi:10.2204/iodp.proc.340.106.2013

Fraass, A. J., Wall-Palmer, D., Leckie, R. M., Hatfield, R. G., Burns, S. J., Le Friant, A., … Talling, P. J. (2016). A revised Plio-Pleistocene age model and paleoceanography of the northeastern Caribbean Sea: IODP Site U1396 off Montserrat, Lesser Antilles. *Stratigraphy*, *13*, 183–203.

Germa, A., Quidelleur, X., Labanieh, S., Chauvel, C., & Lahitte, P. (2011a). The volcanic evolution of Martinique Island: Insights from K-Ar dating into the Lesser Antilles arc migration since the Oligocene. *Journal of Volcanology and Geothermal Research, 208*, 122–135. doi:10.1016/j.jvolgeores.2011.09.007

Germa, A., Quidelleur, X., Labanieh, S., Lahitte, P., & Chauvel, C. (2010). The eruptive history of Morne Jacob volcano (Martinique Island, French West Indies): Geochronology, geomorphology and geochemistry of the earliest volcanism in the recent Lesser Antilles arc. J. Volcanol. Geotherm. Res. 198, 297–310. doi:10.1016/j.jvolgeores.2010.09.013

Germa, A., Quidelleur, X., Lahitte, P., Labanieh, S., & Chauvel, C. (2011b). The K-Ar Cassignol-Gillot technique applied to western Martinique lavas: A record of Lesser Antilles arc activity from 2 Ma to Mount Pelée volcanism. *Quaternary Geochronology, 6*, 341–355. doi:10.1016/j.quageo.2011.02.001

Glicken, H. (1996). Rockslide-debris avalanche of May 18, 1980, Mount St. Helens volcano, Washington. *Open-file Report 96-677*, US Geological Survey.

Hall, P. S., & Kincaid, C. (2001). Diapiric flow at subduction zones: A recipe for rapid transport. *Science, 292*, 2472–2475. doi:10.1126/science.1060488

Harford, C. L., Pringle, M. S., Sparks, R. S. J., & Young, S. R. (2002). The volcanic evolution of Montserrat using $^{40}Ar/^{39}Ar$ geochronology. In Druitt, T. H., & Kokelaar, B. P. (Eds.), *The eruption of the Soufrière Hills volcano, Montserrat from 1995 to 1999* (Vol. 21, pp. 93–113) London: Geological Society Memoirs. doi:10.1144/GSL.MEM.2002.021.01.05

Hart, S. R. (1984). A large-scale isotope anomaly in the Southern Hemisphere mantle. *Nature, 309*, 753–757. doi:10.1038/309753a0

Hatfield, R. G. (2015). Data report: Stratigraphic correlation of Site U1396 and creation of a composite depth scale and splice. In Le Friant, A., Ishizuka, O., Stroncik, N. A., & Expedition 340 scientists. (Eds.) *Proceedings of the Integrated Ocean Drilling Project Program* (Vol. 340) Tokyo: Integrated Ocean Drilling Program Management International, Inc. doi:10.2204/iodp.proc.340.202.2015

Hildreth, W., & Drake, R. E. (1992). Volcán Quizapu, Chilean Andes. *Bulletin of Volcanology, 54*, 93–125. doi:10.1007/BF00278002

Hildreth, W., & Lanphere, M. A. (1994). Potassium-argon geochronology of a basalt-andesite-dacite arc system: The Mount Adams volcanic field, Cascade Range of southern Washington. *Geological Society of America Bulletin, 106*, 1413–1429. doi:10.1130/0016-7606(1994)106<1413:PAGOAB>2.3.CO;2

Hoblitt, R. P., Crandell, D. R., & Mullineaux, D. R. (1980). Mount St. Helens eruptive behavior during the past 1,500 yr. *Geology, 8*, 555–559. doi:10.1130/0091-7613(1980)8<555

Hoshizumi, H., Uto, K., & Watanabe, K. (1999). Geology and eruptive history of Unzen volcano, Shimabara Peninsula, Kyushu, SW Japan. *Journal of Volcanology and Geothermal*

Research, 89, 81–94. doi:10.1016/S0377-0273(98)00125-5

Howe, T. M., Lindsay, J. M., & Shane, P. (2015). Evolution of young andesitic-dacitic magmatic systems beneath Dominica, Lesser Antilles. *Journal of Volcanology and Geothermal Research, 297*, 69–88. doi:10.1016/j.jvolgeores.2015.02.009

Ishizuka, O., Geshi, N., Itoh, J., Kawanabe, Y., & TuZino, T. (2008). The magmatic plumbing of the submarine Hachijo NW volcanic chain, Hachijojima, Japan: Long-distance magma transport? *Journal of Geophysical Research, 113*. doi:10.1029/2007JB005325

Ishizuka, O., Taylor, R. N., Geshi, N., Oikawa, T., Kawanabe, Y., & Ogitsu, I. (2015). Progressive mixed-magma recharging of Izu-Oshima volcano, Japan: A guide to magma chamber volume. *Earth and Planetary Science Letters, 430*, 19–29. doi:10.1016/j.epsl.2015.08.004

Ishizuka, O., Taylor, R. N., Yuasa, M., Milton, J. A., Nesbitt, R. W., Uto, K., & Sakamoto, I. (2007). Processes controlling along-arc isotopic variation of the southern Izu-Bonin arc. *Geochemistry, Geophysics, Geosystems, 8*(6). doi:10.1029/2006GC001475

Kamber, B. S., & Gladu, A. H. (2009). Comparison of Pb Purification by Anion-Exchange Resin Methods and Assessment of Long-Term Reproducibility of Th/U/Pb Ratio Measurements by Quadrupole ICP-MS. *Geostandards and Geoanalytical Research, 33*, 169–181. doi:10.1111/j.1751-908X.2009.00911.x

Kokelaar, B. P. (2002). Setting, chronology and consequences of the eruption of Soufrière Hills Volcano, Montserrat (1995-1999). In Druitt, T. H., & Kokelaar, B. P. (Eds.), *The eruption of the Soufrière Hills volcano, Montserrat from 1995 to 1999* (Vol. 21, pp. 1–43) London: Geological Society Memoirs. doi:10.1144/GSL.MEM.2002.021.01.02

Koleszar, A. M., Kent, A. J. R., Wallace, P. J., & Scott, W. E. (2012). Controls on long-term low explosivity at andesitic arc volcanoes: Insights from Mount Hood, Oregon. *Journal of Volcanology and Geothermal Research, 219–220*, 1–14. doi:10.1016/j.jvolgeores.2012.01.003

Komorowski, J. C., Boudon, G., Smet, M., Beauducel, F., Antenor-Habazac, C., Bazin, S., & Hammouya, G. (2005). Guadeloupe. In Lindsay, J. M. (Ed.), *Volcanic Hazard Atlas of the Lesser Antilles* (pp. 65–102) St Augustine, Trinidad: University of the West Indies.

Labanieh, S., Chauvel, C., Germa, A., & Quidelleur, X. (2012). Martinique: A clear case for sediment melting and slab dehydration as a function of distance to the trench. *Journal of Petrology, 53*, 2441–2464. doi:10.1093/petrology/egs055

Labanieh, S., Chauvel, C., Germa, A., Quidelleur, X., & Lewin, E. (2010). Isotopic hyperbolas constrain sources and processes under the Lesser Antilles arc. *Earth and Planetary Science Letters, 298*, 35–46. doi:10.1016/j.epsl.2010.07.018

Le Friant, A., Harford, C. L., Deplus, C., Boudon, G., Sparks, R. S. J., Herd, R. A., & Komorowski, J. C. (2004). Geomorphological evolution of Montserrat (West Indies): importance of flank collapse and erosional processes. *Journal of the Geological Society of London, 161*, 147–160. doi:10.1144/0016-764903-017

Le Friant, A., Lock, E. J., Hart, M. B., Boudon, G., Sparks, R. S. J., Leng, M., … Fisher, J. K. (2008). Late Pleistocene tephrochronology of marine sediments adjacent to Montserrat,

Lesser Antilles volcanic arc. *Journal of the Geological Society of London, 165*, 279–289. doi:10.1144/0016-76492007-019

Lebas, E., Le Friant, A., Boudon, G., Watt, S. F. L., Talling, P. J., Feuillet, N., … Vardy, M. E. (2011). Multiple widespread landslides during the long-term evolution of a volcanic island: Insights from high-resolution seismic data, Montserrat, Lesser Antilles. *Geochemistry, Geophysics, Geosystems, 12*. doi:10.1029/2010GC003451

Lindsay, J. M., Trumbull, R. B., & Siebel, W. (2005). Geochemistry and petrogenesis of late Pleistocene to Recent volcanism in Southern Dominica, Lesser Antilles. *Journal of Volcanology and Geothermal Research, 148*, 253–294. doi:10.1016/j.jvolgeores.2005.04.018

Macdonald, R., Hawkesworth, C. J., & Heath, E. (2000). The Lesser Antilles volcanic chain: A study in arc magmatism. *Earth Science Reviews, 49*, 1–76. doi:10.1016/S0012-8252(99)00069-0

Macgregor, A. G. (1938). The Royal Society Expedition to Montserrat, B.W.I. The Volcanic History and Petrology of Montserrat, with Observations on Mt Pelée, in Martinique. *Philosophical Transactions of the Royal Society of London. Series B, Biological Sciences, 229*, 1–90.

Mark, D. F., Barfod, D., Stuart, F. M., & Imlach, J. (2009). The ARGUS multicollector noble gas mass spectrometer: Performance for ^{40} Ar/ ^{39}Ar geochronology. *Geochemistry, Geophysics, Geosystems, 10*. doi:10.1029/2009GC002643

Marske, J. P., Pietruszka, A. J., Trusdell, F. A., & Garcia, M. O. (2011). Geochemistry of southern Pagan Island lavas, Mariana arc: The role of subduction zone processes. *Contributions to Mineralogy and Petrology, 162*, 231–252. doi:10.1007/s00410-010-0592-1

Maury, R. C., Westbrook, G. K., Baker, P. E., Bouysse, P., & Westercamp, D. (1990). Geology of the Lesser Antilles. In Dengo, G., & Case, J.E. (Eds.), *The Geology of North America, The Caribbean Region* (Vol. H, pp. 141–166). Boulder, Colorado: Geological Society of America.

Miller, T. P., Chertkoff, D. G., Eichelberger, J. C., & Coombs, M. L. (1999). Mount Dutton volcano, Alaska: Aleutian arc analog to Unzen volcano, Japan. *Journal of Volcanology and Geothermal Research, 89*, 275–301. doi:10.1016/S0377-0273(99)00004-9

Minster, J. B., & Jordan, T. H. (1978). Present-day plate motions. *Journal of Geophysical Research, 83*, 5331–5354. doi:10.1029/JB083iB11p05331

Murphy, M. D., Sparks, R. S. J., Barclay, J., Carroll, M. R., & Brewer, T. S. (2000). Remobilization of Andesite Magma by Intrusion of Mafic Magma at the Soufrière Hills Volcano, Montserrat, West Indies. *Journal of Petrology, 41*, 21–42. doi:10.1093/petrology/41.1.21

Murphy, M. D., Sparks, R. S. J., Barclay, J., Carroll, M. R., Lejeune, A. M., Brewer, T. S., … Young, S. (1998). The role of magma mixing in triggering the current eruption of the Soufrière Hills volcano, Montserrat, West Indies. *Geophysical Research Letters, 25*, 3433–3436. doi:10.1029/98GL00713

Myers, J. D., Marsh, B. D., & Sinha, A. K. (1985). Strontium isotopic and select trace element

variations between two Aleutian volcanic centres (Adak and Atka): Implications for the development of arc volcanic plumbing systems. *Contributions to Mineralogy and Petrology, 91*, 221–234. doi: 10.1007/BF0041334

Odbert, H. M., Ryan, G. A., Mattioli, G. S., Hautmann, S., Gottsmann, J., Fournier, N., & Herd, R. A. (2014). Volcano geodesy at the Soufrière Hills Volcano, Montserrat: a review. In Wadge, G., Robertson, R. E. A., & Voight, B. (Eds.), *The eruption of the Soufrière Hills volcano, Montserrat from 2000 to 2010* (Vol. 39, pp. 195–217) London: Geological Society Memoirs. doi:10.1144/M39.11

Palmer, M. R., Hatter, S. J., Gernon, T. M., Taylor, R. N., Cassidy, M., Johnson, P., … Ishizuka, O. (2016). Discovery of a large 2.4 Ma Plinian eruption of Basse-Terre, Guadeloupe, from the marine sediment record. *Geology, 44*, 123–126. doi:10.1130/G37193.1

Pinel, V., Jaupart, C., & Albino, F. (2010). On the relationship between cycles of eruptive activity and growth of a volcanic edifice. *Journal of Volcanology and Geothermal Research, 194*, 150–164. doi:10.1016/j.jvolgeores.2010.05.006

Pioli, L., Scalisi, L., Costantini, L., Di Muro, A., Bonadonna, C., & Clavero, J. (2015). Explosive style, magma degassing and evolution in the Chaimilla eruption, Villarrica volcano, Southern Andes. *Bulletin of Volcanology, 77*. doi:10.1007/s00445-015-0976-1

Plail, M., Barclay, J., Humphreys, M. C. S., Edmonds, M., Herd, R. A., & Christopher, T. E. (2014). Characterization of mafic enclaves in the erupted products of Soufrière Hills Volcano, Montserrat, 2009 to 2010. In Wadge, G., Robertson, R. E. A., & Voight, B. (Eds.), *The eruption of the Soufrière Hills volcano, Montserrat from 2000 to 2010* (Vol. 39, pp. 343–360) London: Geological Society Memoirs. doi:10.1144/M39.18

Rea, W.J. (1974). The volcanic geology and petrology of Montserrat, West Indies. *Journal of the Geological Society of London, 130*, 341–366. doi:10.1144/gsjgs.130.4.0341

Renne, P. R., Balco, G., Ludwig, K. R., Mundil, R., & Min, K. (2011). Response to the comment by W.H. Schwarz et al. on "Joint determination of ^{40}K decay constants and ^{40}Ar*/^{40}K for the Fish Canyon sanidine standard, and improved accuracy for ^{40}Ar/^{39}Ar geochronology" by P. R. Renne et al. (2010). *Geochimica et Cosmochimica Acta, 75*, 5097–5100. doi:10.1016/j.gca.2011.06.021

Renne, P. R., Mundil, R., Balco, G., Min, K., & Ludwig, K. R. (2010). Joint determination of ^{40}K decay constants and ^{40}Ar*/^{40}K for the Fish Canyon sanidine standard, and improved accuracy for ^{40}Ar/^{39}Ar geochronology. *Geochimica et Cosmochimica Acta, 74*, 5349–5367. doi:10.1016/j.gca.2010.06.017

Ricci, J., Lahitte, P., & Quidelleur, X. (2015a). Construction and destruction rates of volcanoes within tropical environment: Examples from the Basse-Terre Island (Guadeloupe, Lesser Antilles). *Geomorphology, 228*, 597–607. doi:10.1016/j.geomorph.2014.10.002

Ricci, J., Quidelleur, X., & Lahitte, P. (2015b). Volcanic evolution of central Basse-Terre Island revisited on the basis of new geochronology and geomorphology data. *Bulletin of Volcanology, 77: 84*. doi:10.1007/s00445-015-0970-7

Ridolfi, F., Renzulli, A., & Puerini, M. (2010). Stability and chemical equilibrium of amphibole in calc-alkaline magmas: An overview, new thermobarometric formulations and application to subduction-related volcanoes. *Contributions to Mineralogy and Petrology, 160*, 45–66.

doi:10.1007/s00410-009-0465-7

Roobol, M. J., & Smith, A. L. (1998). Pyroclastic stratigraphy of the Soufrière Hills volcano, Montserrat - Implications for the present eruption. *Geophysical Research Letters, 25*, 3393–3396. doi: 10.1029/98GL00643

Roobol, M. J., & Smith, A. L. (1976). Mount Pelée, Martinique: A pattern of alternating eruptive styles. *Geology, 4*, 521–524. doi:10.1130/0091-7613(1976)4<521:MPMAPO>2.0.CO;2

Rose, W. I. (1987). Santa María, Guatemala: bimodal soda-rich calc-alkalic stratovolcano. *Journal of Volcanology and Geothermal Research, 33*, doi:109–129. 10.1016/0377-0273(87)90056-4

Rose, W. I. (1973). Pattern and mechanism of volcanic activity at the Santiaguito Volcanic Dome, Guatemala. *Bulletin of Volcanology, 37*, 73–94. doi:10.1007/BF02596881

Rose, W. I. (1972). Santiaguito Volcanic Dome, Guatemala. *Geological Society of America Bulletin, 83*, 1413–1434. doi:10.1130/0016-7606(1972)83[1413:SVDG]2.0.CO;2

Rowley, K. (1978). Late Pleistocene pyroclastic deposits of Soufrière Volcano, St. Vincent, West Indies. *Bulletin of Geological Society of America, 89*, 825–835. doi:10.1130/0016-7606(1978)89<825:LPPDOS>2.0.CO;2

Ruprecht, P., & Bachmann, O. (2010). Pre-eruptive reheating during magma mixing at Quizapu volcano and the implications for the explosiveness of silicic arc volcanoes. *Geology, 38*, 919–922. doi:10.1130/G31110.1

Samper, A., Quidelleur, X., Komorowski, J.-C., Lahitte, P., & Boudon, G. (2009). Effusive history of the Grande Découverte Volcanic Complex, southern Basse-Terre (Guadeloupe, French West Indies) from new K–Ar Cassignol–Gillot ages. *Journal of Volcanology and Geothermal Research, 187*, 117–130. doi:10.1016/j.jvolgeores.2009.08.016

Samper, A., Quidelleur, X., Lahitte, P., & Mollex, D. (2007). Timing of effusive volcanism and collapse events within an oceanic arc island: Basse-Terre, Guadeloupe archipelago (Lesser Antilles Arc). *Earth and Planetary Science Letters, 258*, 175–191. doi:10.1016/j.epsl.2007.03.030

Scott, W. E., Pierson, T. C., Schilling, S. P., Costa, J. E., Gardner, C. A., Vallance, J. W., & Major, J. J. (1997). Volcano Hazards in the Mount Hood Region, Oregon. *Open-File Report 1–14*, US Geological Survey.

Siebert, L. (1984). Large volcanic debris avalanches: Characteristics of source areas, deposits, and associated eruptions. *Journal of Volcanology and Geothermal Research, 22*, 163–197. doi:10.1016/0377-0273(84)90002-7

Smith, A. L., Roobol, M. J., Mattioli, G. S., Fryxell, J. E., Daly, G. E., & Fernandez, L. A. (2013). *The volcanic geology of the mid-arc island of Dominica, Lesser Antilles*. Boulder, Colorado: Geological Society of America.

Smith, A. L., Roobol, M. J., Schellekens, J. H., & Mattioli, G. S. (2007). Prehistoric stratigraphy of the Soufrière Hills-South Soufrière Hills volcanic complex, Montserrat, West Indies. *Geology, 115*, 115–127. doi:10.1086/509271

Sparks, R. S. J., Barclay, J., Calder, E. S., Herd, R. A., Komorowski, J.-C., Luckett, R., …

Woods, A. W. (2002). Generation of a debris avalanche and violent pyroclastic density current on 26 December (Boxing Day) 1997 at Soufrière Hills Volcano, Montserrat. In Druitt, T. H., & Kokelaar, B. P. (Eds.), *The eruption of the Soufrière Hills volcano, Montserrat from 1995 to 1999* (Vol. 21, pp. 409–434) London: Geological Society Memoirs. doi:10.1144/GSL.MEM.2002.021.01.18

Sparks, R. S. J., Folkes, C. B., Humphreys, M. C. S., Barfod, D. N., Clavero, J., Sunagua, M. C., … Pritchard, M. E. (2008). Uturuncu volcano, Bolivia: Volcanic unrest due to mid-crustal magma intrusion. *American Journal of Science, 308*, 727–769. doi:10.2475/06.2008.01

Stern, R. J. (2002). Subduction zones. *Reviews of Geophysics, 40*. doi:10.1029/2001RG000108

Stinton, A. J., Cole, P. D., Stewart, R. C., Odbert, H. M., & Smith, P. (2014). The 11 February 2010 partial dome collapse at Soufrière Hills Volcano, Montserrat. In Wadge, G., Robertson, R. E. A., & Voight, B. (Eds.), *The eruption of the Soufrière Hills volcano, Montserrat from 2000 to 2010* (Vol. 39, pp. 133–152) London: Geological Society Memoirs. doi:10.1144/M39.7

Takarada, S., Ui, T., & Yamamoto, Y. (1999). Depositional features and transportation mechanism of valley-filling Iwasegawa and Kaida debris avalanches. *Japanese Bulletin of Volcanology, 60*, 508–522. doi:10.1007/s004450050248

Taylor, R. N., Ishizuka, O., Michalik, A., Milton, J. A., & Croudace, I. W. (2015). Evaluating the precision of Pb isotope measurement by mass spectrometry. *Journal of Analytical Atomic Spectrometry, 30*, 198–213. doi:10.1039/C4JA00279B

Toothill, J., Williams, C. A., MacDonald, R., Turner, S. P., Rogers, N. W., Hawkesworth, C. J., … Tindle, A. G. (2007). A complex petrogenesis for an arc magmatic suite, St Kitts, Lesser Antilles. *Journal of Petrology, 48*, 3–42. doi:10.1093/petrology/egl052

Ui, T. (1983). Volcanic dry avalanche deposits — Identification and comparison with nonvolcanic debris stream deposits. *Journal of Volcanology and Geothermal Research, 18*, 135–150. doi:10.1016/j.jvolgeores.2008.06.025

Ui, T., & Glicken, H. (1986). Internal structural variations in a debris-avalanche deposit from ancestral Mount Shasta, California, USA. *Bulletin of Volcanology, 48*, 189–194. doi:10.1007/BF01087673

Ui, T., Kawachi, S., & Neall, V. E. (1986). Fragmentation of debris avalanche material during flowage — Evidence from the Pungarehu Formation, Mount Egmont, New Zealand. *Journal of Volcanology and Geothermal Research, 27*, 255–264. doi:10.1016/0377-0273(86)90016-8

van Wyk de Vries, B., & Davies, T. (2015). Landslides, Debris Avalanches and Volcanic Gravitational Deformation. In: Sigurdsson, H., Houghton, B., McNutt, S. R., Rymer, H., Stix, J. (Eds.), *The Encylopedia of Volcanoes, 2nd edition* (pp. 665–685). Elsevier Inc.

Venezky, D. Y., & Rutherford, M. J. (1999). Petrology and Fe–Ti oxide reequilibration of the 1991 Mount Unzen mixed magma. *Journal of Volcanology and Geothermal Research, 89*, 213–230. doi:10.1016/S0377-0273(98)00133-4

Voight, B., Komorowski, J.-C., Norton, G. E., Belousov, A. B., Belousova, M., Boudon, G., … Young, S. R. (2002). The 26 December (Boxing Day) 1997 sector collapse and debris

avalanche at Soufrière Hills Volcano, Montserrat. In Druitt, T. H., & Kokelaar, B. P. (Eds.), *The eruption of the Soufrière Hills volcano, Montserrat from 1995 to 1999* (Vol. 21, pp. 363–407) London: Geological Society Memoirs. doi:10.1144/GSL.MEM.2002.021.01.17

Wadge, G., Voight, B., Sparks, R. S. J., Cole, P. D., Loughlin, S. C., & Robertson, R. E. A. (2014). An overview of the eruption of Soufrière Hills Volcano, Montserrat from 2000 to 2010. In Wadge, G., Robertson, R. E. A., & Voight, B. (Eds.), *The eruption of the Soufrière Hills volcano, Montserrat from 2000 to 2010* (Vol. 39, pp. 1–40) London: Geological Society Memoirs. doi:10.1144/M39.1

Wendt, I., & Carl, C. (1991). The statistical distribution of the mean squared weighted deviation. *Chemical Geology: Isotope Geoscience Section*, *86*, 275–285. doi:10.1016/0168-9622(91)90010-T

Westercamp, D., & Traineau, H. (1983). The past 5,000 years of volcanic activity at Mt. Pelée Martinique (F.W.I): Implications for assessment of volcanic hazards. *Journal of Volcanology and Geothermal Research, 17*, 159–185. doi: 10.1016/0377-0273(83)90066-5

White, J. D. L., & Houghton, B. F. (2006). Primary volcaniclastic rocks. *Geology, 34*, 677–680. doi:10.1130/G22346.1

Wohletz, K., Heiken, G., Ander, M., Goff, F., Vuataz, F.-D., & Wadge, G. (1986). The Qualibou caldera, St. Lucia, West Indies. *Journal of Volcanology and Geothermal Research, 27*, 77–115. doi:10.1016/0377-0273(86)90081-8

Wright, J. V., Roobol, M. J., Smith, A. L., Sparks, R. S. J., Brazier, S.A., & Rose, W. I., Sigurdsson, H. (1984). Late Quaternary explosive silicic volcanism on St Lucia, West Indies. *Geological Magazine*, *121*, 1–15. doi:10.1017/S0016756800027904

Young, S. R., Hoblitt, R. P., Smith, A. L., Devine, J. D., Wadge, G., & Shepherd, J. B. (1996). *Dating of explosive volcanic eruptions associated with dome growth at the Soufrière Hills volcano, Monserrat, West Indies*. Paper presented at 2nd Caribbean Conference on Natural Hazards and Hazard Management, Kingston.

Table 1. Compiled literature $^{40}Ar/^{39}Ar$ dates on Montserrat. Ages from Harford et al. (2002) and Brown and Davidson (2008) presented here are recalculated ages (see text for details).

Sample	Rock type	Location/unit	Grid reference mE mN	Material	Plateau age (ka)	±2σ	MSWD	N	% ^{39}Ar
MVO144[1]	Lava	Silver Hill	378025 1857050	Plagioclase	2614[m]	121	0.69	7/11	65.3
SH07-F[2]	Lava	Yellow Hole	380408 1857634	Groundmass	**1520**[i]	**51**	0.58	7/7	100.0
SH07-C[2]	Lava	Drummonds	379033 1857296	Groundmass	**1430**[i]	**19**	1.09	7/7	100.0
SH07-D[2]	BAF	Drummonds	378873 1857117	Groundmass	**1412**[i]	**20**	0.66	7/8	>95.0
SH07-B[2]	BAF	Silver Hill	379081 1857776	Groundmass	**1397**[i]	**20**	0.46	7/7	100.0
SH07-E[2]	Lava	Drummonds	378859 1857000	Groundmass	**1395**[i]	**17**	0.82	7/7	100.0
11.1.4C[3]	PAF	South Lime Kiln Bay	374681 1851092	Plagioclase	**1310**	**200**	0.95	6/7	
MVO755[1]	Lava	Silver Hill	378650 1856400	Groundmass	1192[r]	95	20.79[e]	5/16	64.6
MVO135[1]	s-BAF	Roche's Bluff	383975 1846150	Whole-rock	1051	40	4.37[e]	7/14	62.1
MOV148[1]	Lava	Harris	382150 1850450	Whole-rock	982[m,r]	24	4.99[e]	10/12	93.0
MVO131[1]	Lava	Trant's	382050 1851975	Whole-rock	**896**	**20**	1.40	12/12	100.0
MVO831[1]	BAF	Lower Centre Hills	381763 1853525	Groundmass	850	24	2.01[e]	9/14	73.7
BP[3]	PF	Bransby Pumice	374092 1848396	Plagioclase	**790**	**170**	0.87	6/7	
4.2.3G[3]	PAF	Old Road Bay	374638 1848989	Plagioclase	**700**	**140**	0.88	5/6	
MVO147[1]	PAF	Upper Centre Hills	377600 1855050	Plagioclase	683[m]	98	0.93	5/12	76.4
3.1.2A[3]	PAF	Woodlands Bay	375879 1852755	Plagioclase	**590**	**110**	1.14	7/7	100.0
MVO809[1]	BAF	Upper Centre Hills	381475 1853750	Groundmass	**566**	**45**	1.01	14/14	100.0
3.4.2H[3]	PAF	Bunkum Bay	376014 1853421	Plagioclase	**510**	**110**	0.41	5/7	
3.1.8C[3]	PAF	Attic	375951 1853042	Plagioclase	**480**	**200**	0.99	3/8	
MVO785[1]	BAF	Garibaldi Hill	374990 1850025	Groundmass	**290**	**16**	0.15	6/15	66.7
MVO819[1]	—	SH-1[4]	383238 1849275	Groundmass	182	10	2.48[e]	5/10	91.5
				Groundmass	178	6	1.03	5/9	66.7
				Composite	**179**	**6**	0.53		
MVO152[1]	Lava	Gages Dome	379275 1847175	Whole-rock	230	14	0.23	5/14	53.6
				Groundmass	163	12	3.23	2/10	53.7
				Groundmass	153	6	1.06	5/9	64.2
				Composite	**155**	**8**	1.84		
MVO139[1]	Lava	Landing Bay	383950 1845000	Whole-rock	142	18	1.28	5/11	61.1
				Groundmass	128	18	2.89[e]	14/17	87.1
				Composite	**135**	**14**	1.13		
MVO136[1]	Lava	Roche's Bluff	384250 1845650	Whole-rock	134[i,x]	10	0.79	10/11	97.4
MVO830[1]	Breccia	Roche's Bluff	383975 1845050	Groundmass	**133**	**34**	0.64	8/16	76.0
MVO791[1]	Lava	Shoe Rock	381600 1843150	Groundmass	**133**	**28**	0.35	6/10	70.7
MVO1099[1]	—	SSH-F[4]	379750 1844325	Groundmass	157	18	1.00	6/9	55.5
				Groundmass	102	20	0.45	3/9	63.0
				Composite	132	55	16.67[e]		
18654[1]	Lava	Galway's Dome	—	Groundmass	124	8	1.96	5/10	58.2
				Groundmass	106	10	0.52	4/10	59.4
				Composite	115	18	8.45[e]		
MVO777[1]	—	SH-II[4]	383675 1847250	Groundmass	86	10	1.23	3/8	63.2
				Groundmass	66	12	0.33	3/9	60.4
				Composite	77	20	6.53[e]		
MVO149[1]	Lava	Chances Dome	379900 1846825	Whole-rock	40[r]	26	15.9[e]	4/11	54.2
MVO127[1]	—	SH-III[4]	383550 1849975	Groundmass	**39**	**16**	0.13	3/10	72.5

MVO154[1]	Lava	Perches Dome	382100 1846750	Whole-rock	33	8	1.61	5/11	65.3
				Groundmass	25	4	0.54	5/9	65.9
				Groundmass	24	6	0.20	4/10	68.3
				Composite	**25**	**4**	0.18		
MVO775[1]	—	SH-III[4]	383425 1847675	Groundmass	**25**	**2**	0.93	4/9	64.0
MVO104[1]	BAF	1996 Dome	—	Groundmass	**22**	**44**	0.25	4/10	63.8
				Plagioclase	439	192	3.26[e]	7/10	71.1

[1] Harford et al. (2002); [2] Brown and Davidson (2008); [3] Coussens et al. (2017); [4] unit name from Smith et al. (2007). BAF, block-and-ash flow deposit; PAF, pumice-and-ash flow deposit; S-BAF, submarine-BAF; PF, pumice fall deposit. Ages considered reliable are in bold. Ages viewed with caution: [m] maximum age; [r] Ar recoil; [x] excess Ar; [e] MSWD exceeds critical value. [i] isochron age. N, number of plateau steps used to determine age/total number of steps; %^{39}Ar, percentage of total ^{39}Ar in N.

Table 2. New $^{40}Ar/^{39}Ar$ dates for the Silver Hills, Centre Hills and Soufrière Hills.

Sample	Rock type	Location/unit	Grid reference mE mN	Material	Isochron age (ka)	±2σ	$^{40}Ar/^{36}Ar_{(i)}$	±2σ	MS WD	Plateau age (ka)	±2σ	MS WD	N	% ^{39}Ar	^{39}Ar (mol)	Ca/K
22/84-AC	BAF	South Silver Hill	378940 1856619	Plagioclase	2160	200	300.6	8.4	1.20	2220	220	1.08	8/12	84.8	5.3E-17	105
				Plagioclase	2300	630	290.0	23.0	1.50	2110	210	1.38	7/12	96.2	4.1E-17	99
				Composite	2140	260	299.5	8.0	1.30	**2170**	**180**	1.19	15/24		9.5E-17	103
14/25-AL	Lava	Marguerita Ghaut	380235 1857105	Plagioclase	1680	230	298.6	8.3	1.20	**1682**	**94**	0.99	6/10	90.5	8.4E-17	76
15/70-AC	BAF	North Marguerita Bay	380310 1856978	Groundmass	1580	140	298.2	0.4	0.71	1630	140	0.71	6/12	77.6	6.6E-16	5
				Plagioclase	1710	260	302.0	24.0	1.20	1770	210	1.11	11/12	99.6	6.1E-17	135
				Composite	1640	80	298.2	0.67	1.20	**1634**	**83**	1.06	17/24		7.2E-16	123
22/47-AL	Lava	North West Bluff	378130 1859071	Plagioclase	1550	130	293.0	13.0	0.97	**1493**	**98**	0.95	11/12	99.4	8.3E-17	79
20/42-AC	MF	Thatch Valley	379710 1858870	Plagioclase	1340	140	302.2	3.8	1.20	**1450**	**160**	1.13	11/12	99.8	5.6E-17	107
11/09-AL	LMB	Culture Hill	378378 1856630	Plagioclase	1510	180	296.5	30	0.49	**1430**	**120**	0.54	10/13	94.2	1.0E-16	64
17/77-AL	Lava	North Rendezvous Bay	377754 1858327	Plagioclase	1260	330	305.0	12.0	1.00	**1424**	**80**	1.17	8/11	99.1	1.1E-16	54
12/13-AC	BAF	South Marguerita Bay	380452 1856780	Plagioclase	1250	350	306.0	16.0	1.10	1390	220	1.04	8/10	98.9	3.7E-17	127
				Plagioclase	1520	780	285.0	25.0	1.10	1160	360	1.04	7/12	88.3	2.0E-17	130
				Composite	1360	280	297.0	13.0	1.10	**1330**	**190**	1.05	15/22		5.7E-17	128
17/76-AL	Lava	Little Bay Quarry	378449 1857434	Plagioclase	Excess ^{40}Ar					No resolvable plateau						
				Plagioclase	1250	440	296.0	13.0	0.54	1180[n]	300	0.50	9/13	62.6	3.0E-17	93
21/81-AC	BAF	East Centre Hills	381671 1853642	Plagioclase	1020	390	301.0	13.0	0.67	**1040**	**250**	0.62	12/12	100.0	5.3E-17	123
05/03-AL	Lava	Dry Waterfall	378605 1852689	Groundmass	370	20	308.0	14.0	1.80	377	18	1.67	11/13	89.8	1.0E-15	6
				Plagioclase	530	90	290.8	8.9	0.37	406	69	0.59	8/12	95.8	1.2E-16	54
				Composite	376	18	299.5	3.8	1.30	**378**	**18**	1.20	19/25		1.1E-15	53
28/57-AC	BAF	Spring Ghaut	376605 1850521	Plagioclase	400	140	298.3	3.7	1.20	392	98	1.04	8/11	95.0	7.3E-17	79
				Plagioclase	240	340	300.4	4.8	0.53	330	170	0.54	7/10	96.9	5.2E-17	74
				Composite	360	110	298.9	2.1	0.84	**376**	**85**	0.78	15/21		1.2E-16	77
Pumice samples					**Probability density Function Age (ka)**											
23/86-PF	PF	Potato Hill	377806 1856742	Plagioclase						**800**	**120**	1.03	15/19			107
20/79-PC	PAF	South Centre Hills	376612 1850198	Plagioclase						**450**	**170**	0.79	9/15			84
16/72-PR	r-PF	Old Quaw Ghaut	380443 1857979	Plagioclase						**450**	**130**	1.23	14/18			66

Abbreviations same as Table 2. MF, debris avalanche deposit matrix facies; LMB, lava megablock within debris avalanche deposit; r-PF, reworked-PF. Preferred ages for this study in bold. [n] age from non-reproducible release spectra. See supplementary Table 2 for decay rates, isotopic constants and nucleogenic production ratios.

1108

Table 3. Lithofacies abbreviations used. Adapted from Branney and Kokelaar (2002). m-dsLT_{lensBr}, for example, means massive to diffuse-stratified lapilli-tuff with lenses of breccia.

Symbol	Lithofacies
T	Tuff
LT	Lapilli-tuff
TBr	Tuff-breccia
Br	Breccia
m	Massive
p	Pumice-rich
ds	Diffuse-stratified
//s	Parallel-stratified
$_{(n)}$	Normal-graded
$_{(i)}$	Inverse-graded
$_{lensBr}$	Lens(es) of breccia
$_{MB}$	Megablock

Table 4. Tephra layers in core U1396C spanning the time interval 2.35–0.37 Ma.

Tephra layer	Age (Ma)	Provenance	Pumice?*
2H1W-66/81	0.63	Centre Hills	Yes
2H2W-39.5/52	0.70	Centre Hills	Yes
2H2W-148.5/ 2H3W-14	0.77	Centre Hills	No
2H4W-94.5/98	0.86	Centre Hills	No
2H7W-62.5/67	1.02	Centre Hills	TF
3H1W-10/12	1.03	Silver Hills	Yes
3H1W-24/27.5	1.03	Guadeloupe	Yes
3H1W-50.5/53	1.04	Centre Hills	NVL
3H2W-23.5/26	1.08	Centre Hills	Yes
3H2W-58/67	1.10	Silver Hills	Yes
3H2W-142.5/149	1.14	Centre Hills	Yes
3H6-32/37	1.41	Guadeloupe	Yes
3H7W-33/40	1.49	Silver Hills	TF
4H2W-29/32	1.62	Silver Hills	Yes
4H6W-42/44	1.88	Silver Hills	Yes

*Contains enough pumice for geochemical analysis. TF, too fine-grained to separate pumice from the other components; NVL, fresh non-vesicular lava grains analysed.

Figure Captions

Figure 1: (a) Map of the Lesser Antilles, showing the location of IODP Expedition 340 core site U1396. (b) Map of Montserrat with bathymetry (100 m intervals), showing the location of the volcanic centers and $^{40}Ar/^{39}Ar$ dates. Pale areas with horizontal stripes are uplifted regions. Orange areas with diagonal stripes within the Soufrière Hills show the locations of the lava domes: 1, Chances Peak; 2, Gages Mountain; 3, Galway's Mountain; 4, Perches Mountain; 5, Castle Peak. Dot-dashed line shows edge of English's Crater. White dots mark the locations of Soufrières, which are (from left to right): Gages Lower, Gages Upper, Galway's and Tar River. Accepted ages in bold. Ages viewed with caution: ^{m} maximum age; ^{r} Ar recoil; ^{x} excess Ar; ^{e} MSWD exceeds critical value; see text for details.

Figure 2: Exposure map of Silver Hills with locations of $^{40}Ar/^{39}Ar$ dates and stratigraphic logs. Accepted ages in bold. Ages viewed with caution: ^{m} maximum age; ^{e} MSWD exceeds critical value; ^{n} age from non-reproducible release spectra; see text for details. Contour spacing is 100 feet. Bold contours are every 500 feet. British West Indies Grid; each grid square is 1 km^2.

Figure 3: Plateau age diagrams for the twelve lava samples. Ages in Ma ± 2σ.

Figure 4: Age-probability spectra for the three pumice samples. Dotted lines show spectra including all data, solid lines show spectra after data rejection. Data at 1σ, results at 2σ, ages in Ma ± 2σ. Includes error in J. Filtering: nMAD = 1.5.

Figure 5: (a) Sketch of exposure along north Marguerita Bay, showing the relationship between units. Heavy black line = joint. (b) Southern corner of the exposure shown in (a), showing unit MB8 (left) cutting down through units MB3–4 (right). (c) Interdigitation of units MB4 and MB5. (d) Mingled boundary between units MB8 (grey) and MB9 (golden brown), with isolated blocks of MB8 floating in MB9. See supplementary material for unit descriptions.

Figure 6: (a) Stratigraphic log from log site 1 at the top of Potato Hill. Units PH2 and 4 are the poorly-sorted sub-facies, unit PH3 is well-sorted sub-facies. (b) Stratigraphic logs from log sites 2 (left) and 3 (right) in Old Quaw Ghaut. Note the significant variation between the two sites, just ~60 m apart. Black clasts represent andesite, orange clasts hydrothermally altered andesite, white clasts pumice.

Figure 7: Pb isotopes showing separation between the South Soufrière Hills, Soufrière Hills and Centre and Silver Hills. Δ7/4 is $^{207}Pb/^{204}Pb$ calculated to the Northern Hemisphere Reference Line (Hart, 1984).

Figure 8. Nb/Y vs 143Nd/144Nd separating between Silver and Centre Hills. (a) Terrestrial samples, and identifying the provenance of samples with uncertain origin: SMB, South Marguerita Bay; LKB, Lime Kiln Bay; DH, Davy Hill; PH, Potato Hill. (b) Marine tephra samples from core U1396C. Numbers note age of tephra layers in Ma. Faded terrestrial samples are shown for comparison.

Figure 9: Thin section images of andesite lava and enclave textures, and boundaries between them.

Figure 10: Schematic map-view evolution of the Silver Hills volcanic center. Active domes and their associated deposits are in bold.

Figure 11: Timing of volcanic activity on Montserrat. Colored bands define our revised timings of volcanism for the different volcanic centers. All literature ages are shown for comparison. Literature ages from Harford et al. (2002); Brown and Davidson, (2008); Coussens et al. (2017).

Figure S1: Block-and-ash flow deposits (units V2–4) by Valentine Hill.

Figure S2: (a) Highly fractured andesite lava, east of Potato Hill, which is locally brecciated (b). Notebook for scale is 19 x 12 cm.

Figure S3: (a) Field sketch of a road cutting at GR 378001 1856419 (road to Davy Hill) showing a pyroclastic sequence (units DH1–4) filling a channel in hydrothermally altered lava. Facing SSW. (b) Single-unit volcaniclastic megablock of stratified tuff, and (c) sheared single-unit volcaniclastic megablocks of tuff, within unit DH5 (highlighted by black lines).

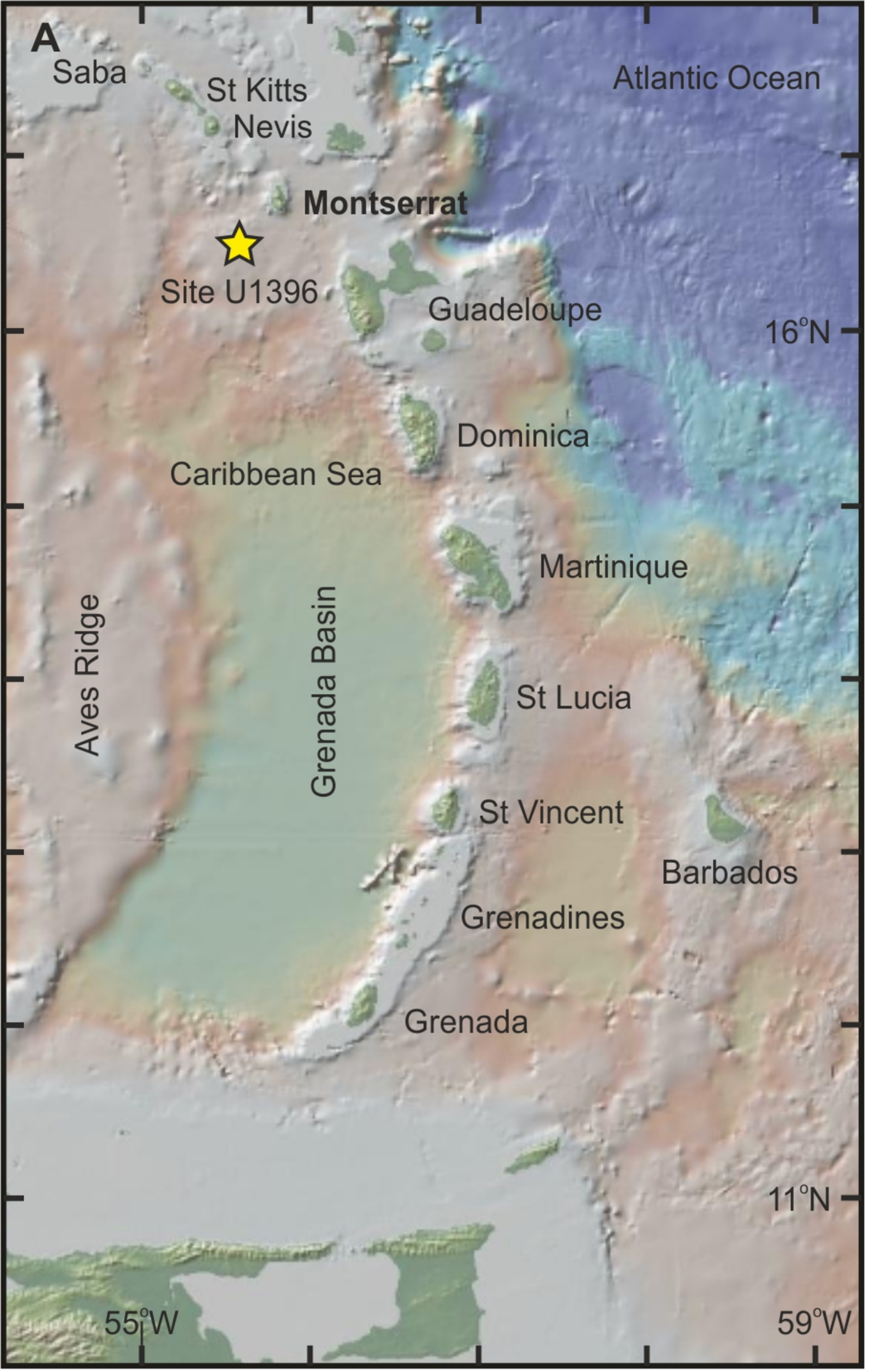

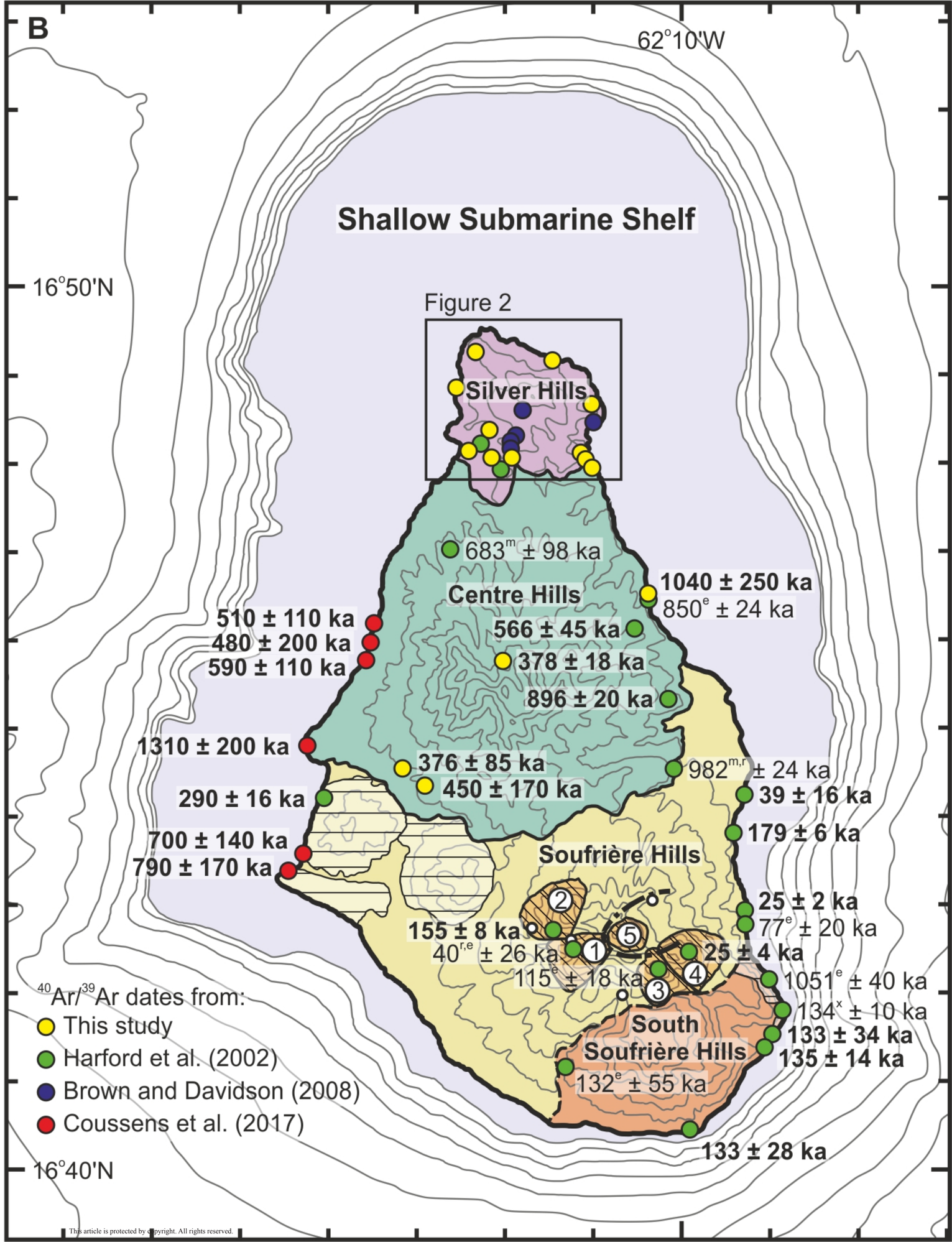

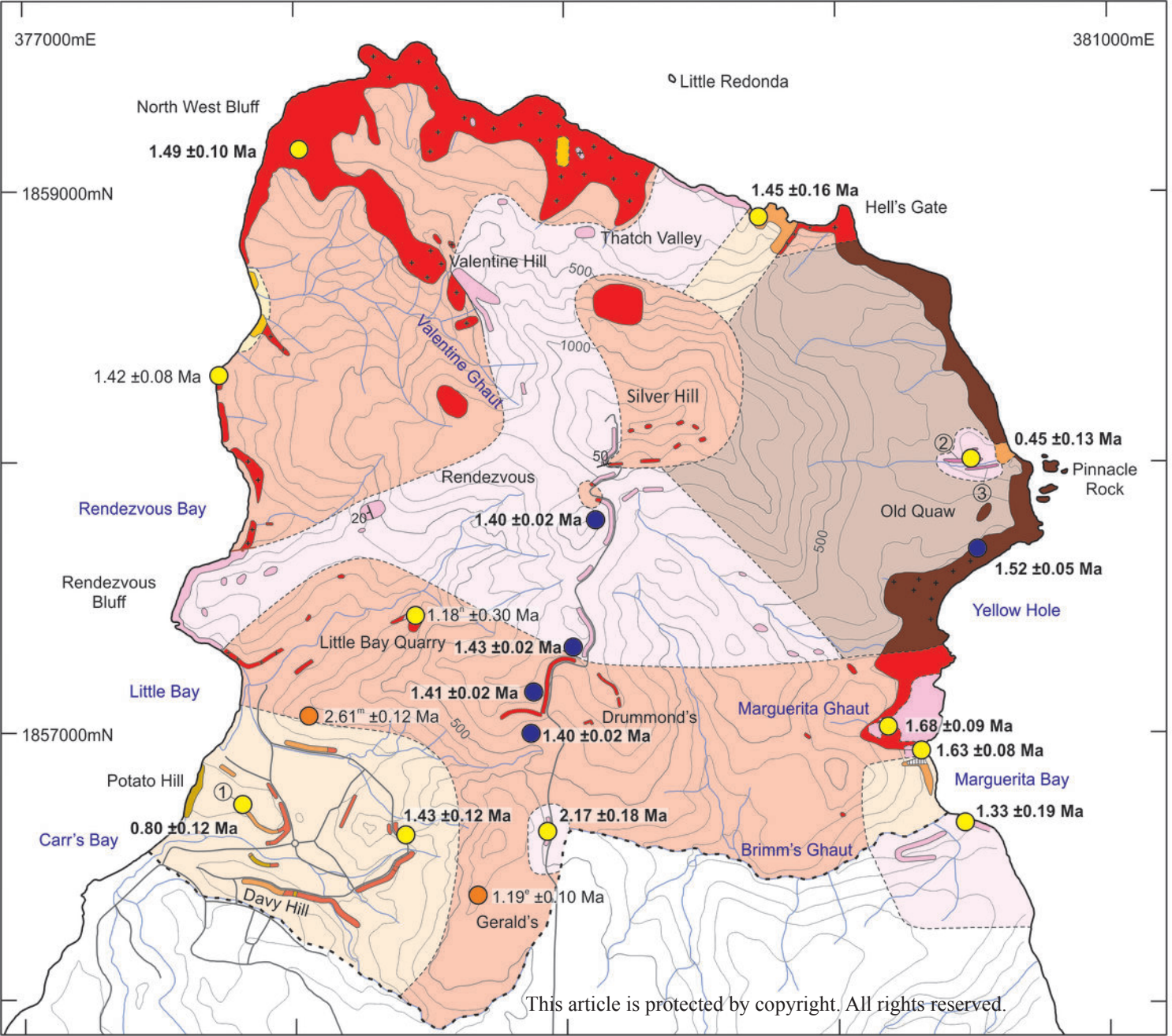

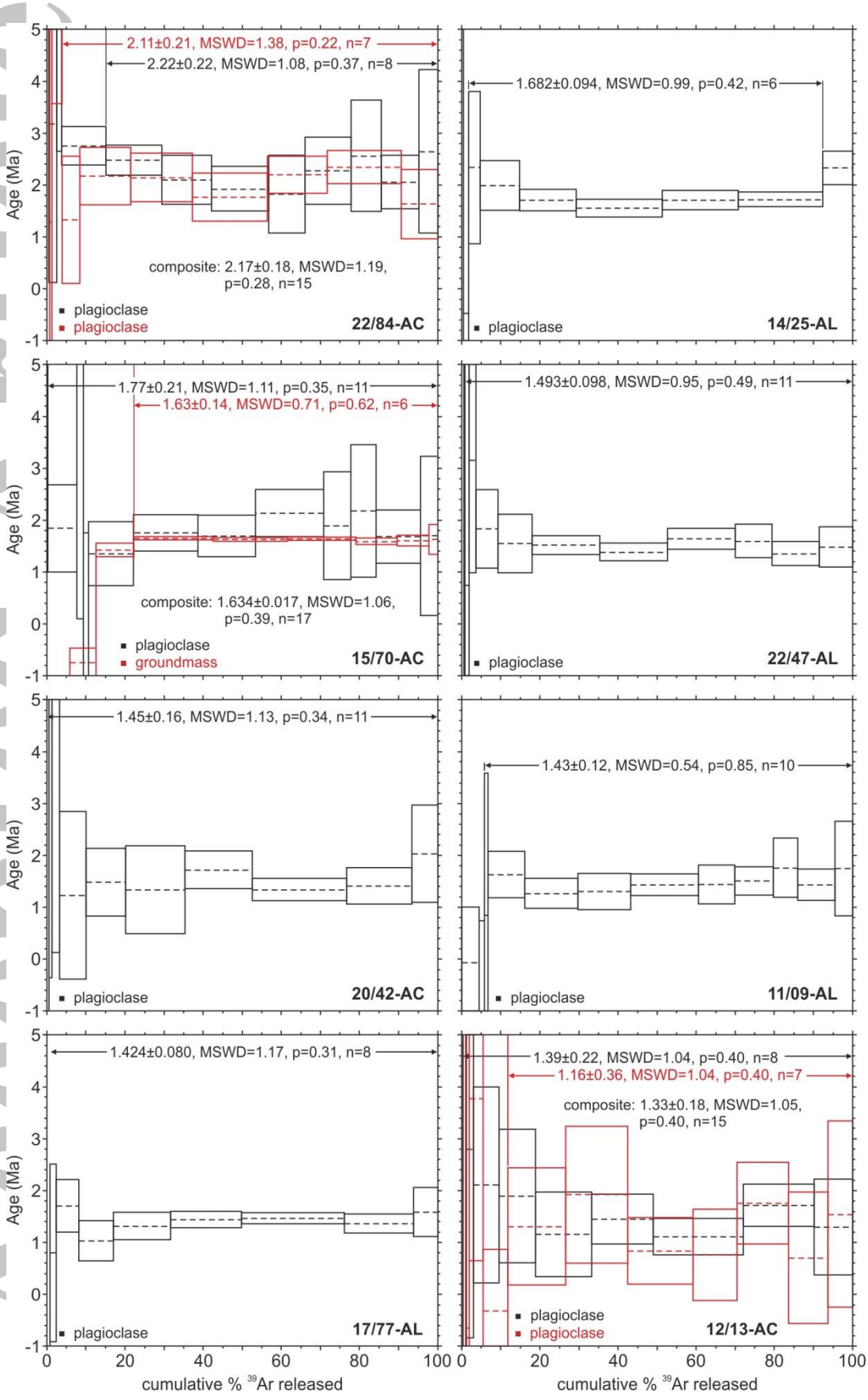

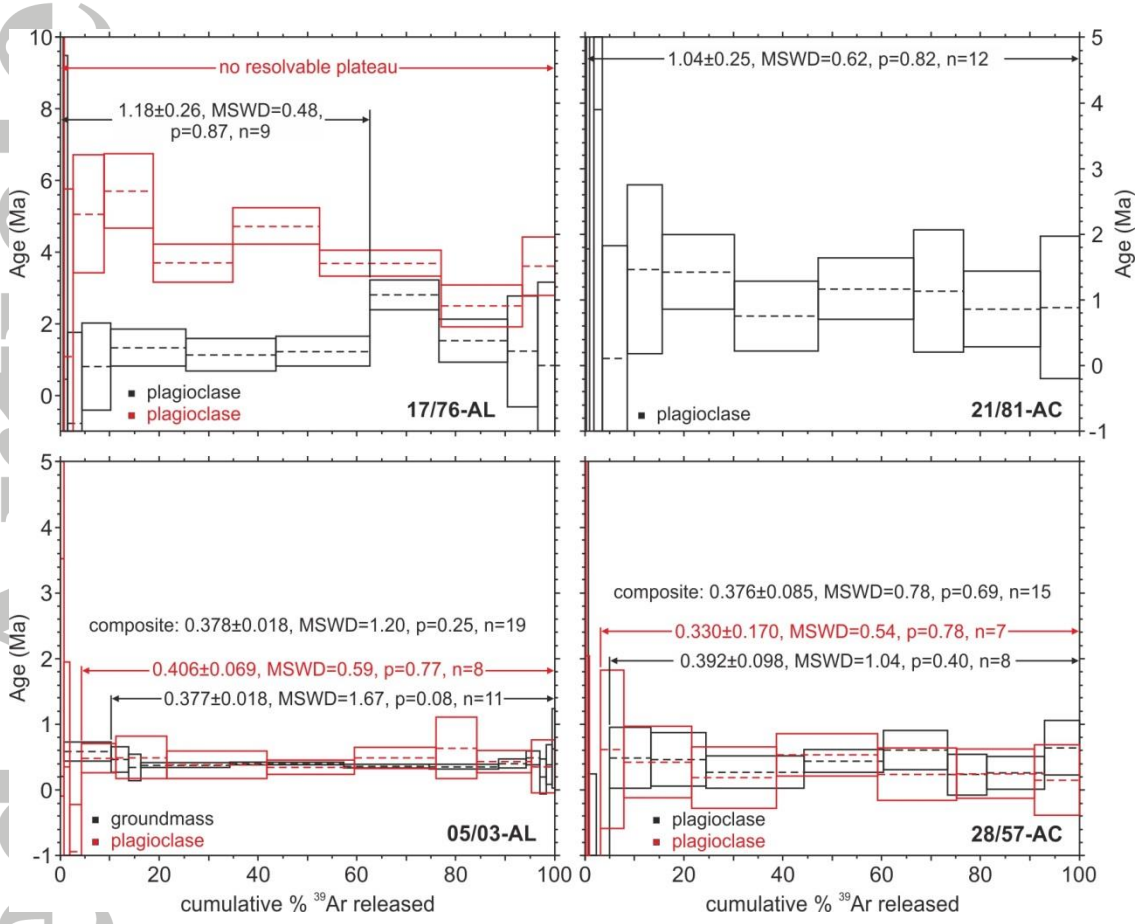

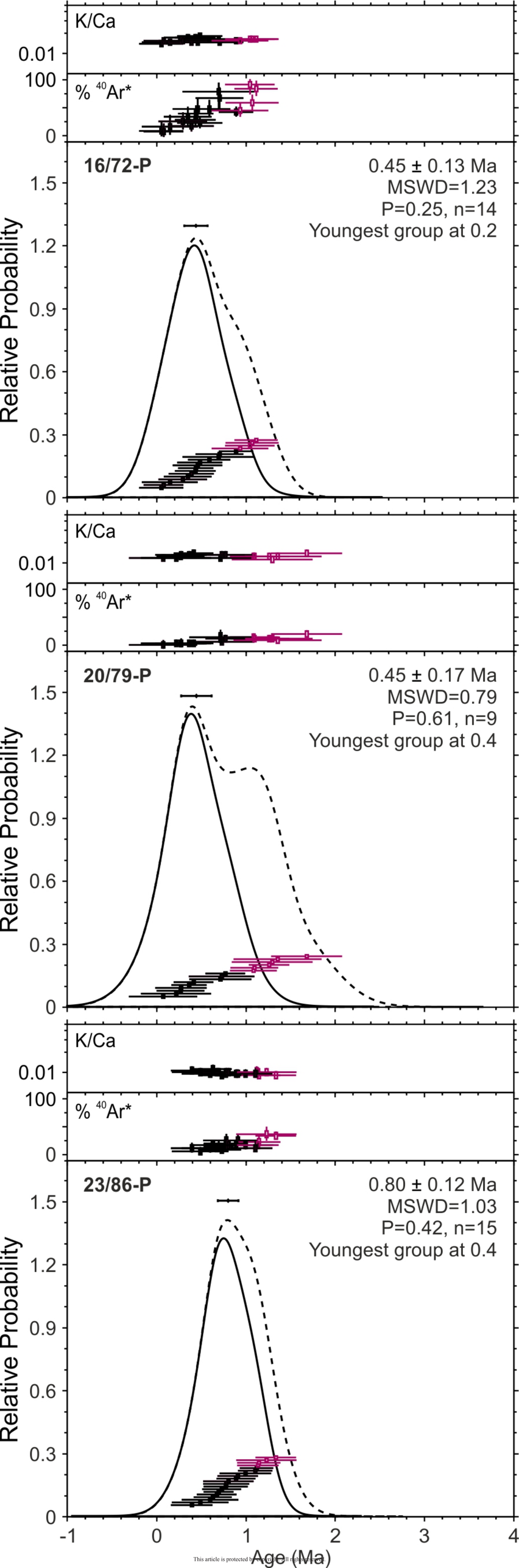

A

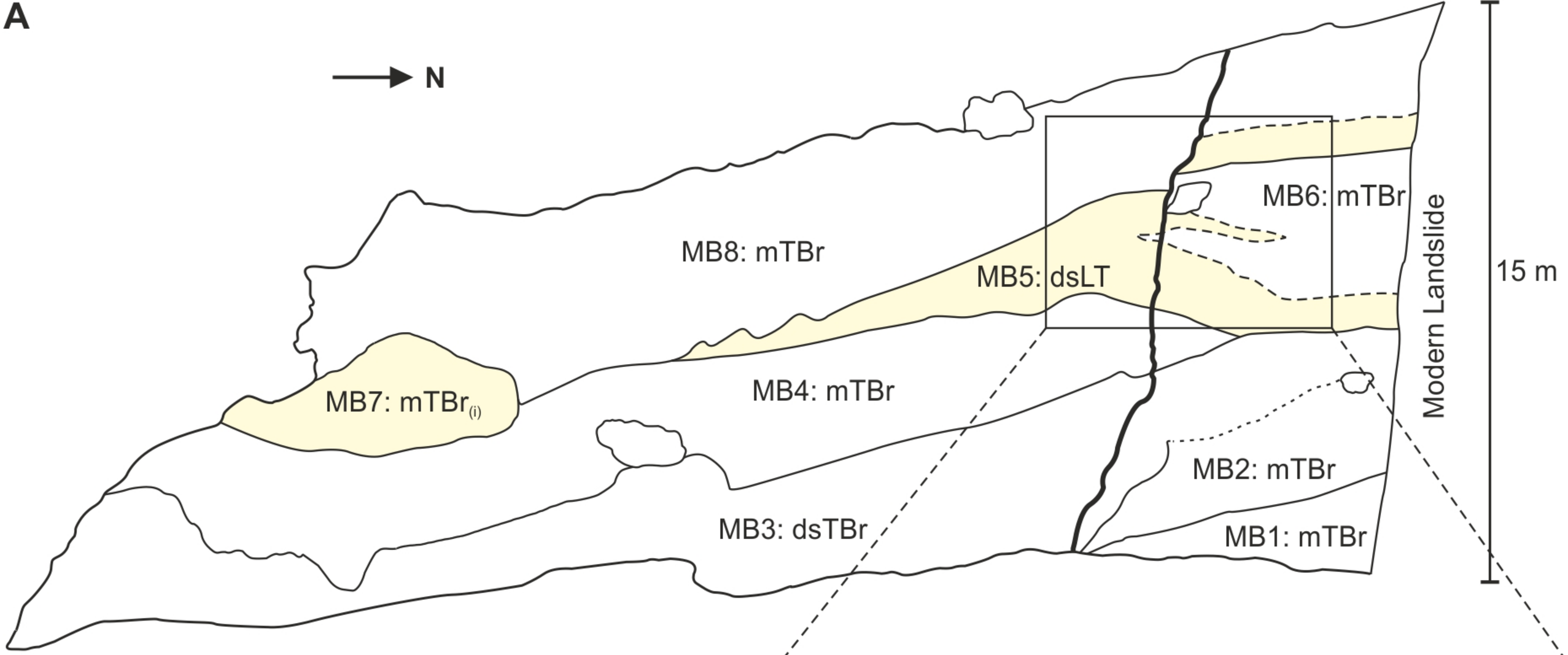

B

C

D

A

m

6

5

4

3

2

1

PH4

PH3

PH2

pmTBr$_{ps}$

pmLT$_{ps}$

pLT$_{ws}$

pmTBr$_{ps}$

pmLT$_{ps}$

pmTBr$_{ps}$

2 64 mm

Ash Lapilli Blocks

B

m

10

9

8

7

6

5

pmLT

lensBr

pmLT$_{(n)}$

pmTBr

OQ3a

pmLT

pmLT

OQ3b

OQ2c

OQ2a

OQ1

mLT$_{lensLT-TBr}$

Continues the same for 5 m

2 64 mm

Ash Lapilli Blocks

m

3

2

OQ4

OQ2b 1

Interbedded T and pLT

pmCLT

pmLT

//sT

pmLT$_{(i)}$

mLT$_{lensLT-TBr}$

2 64 mm

Ash Lapilli Blocks

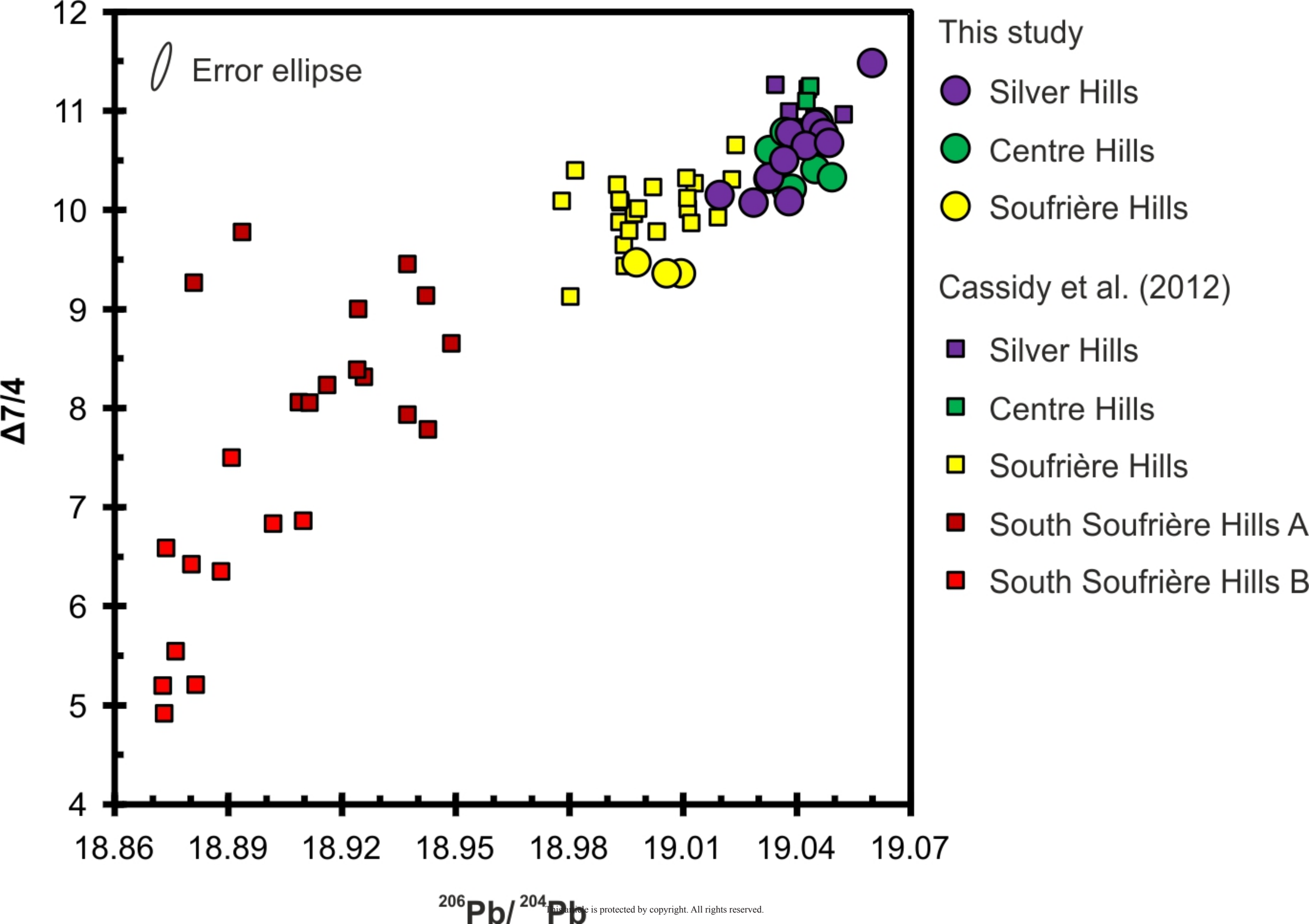

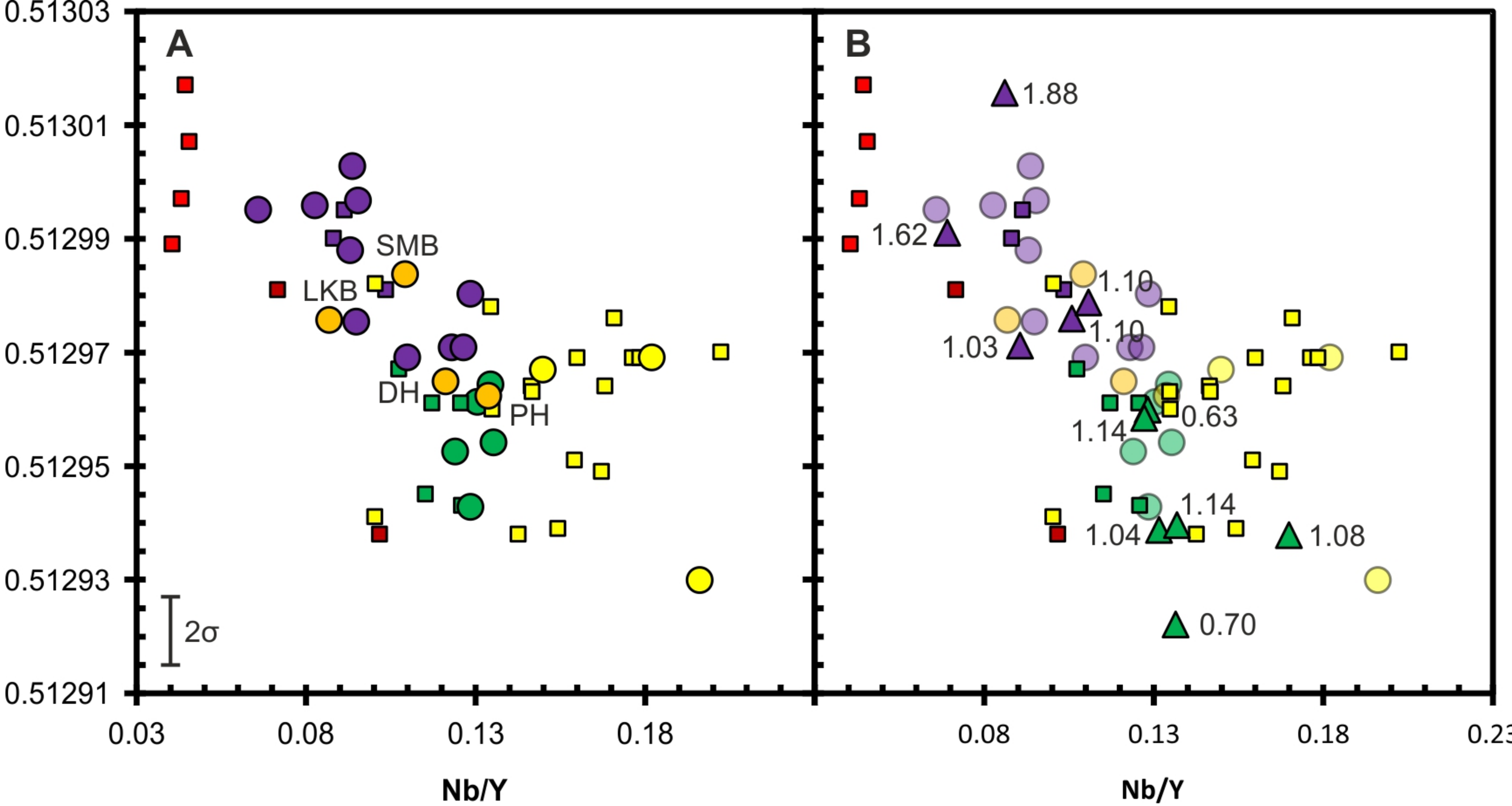

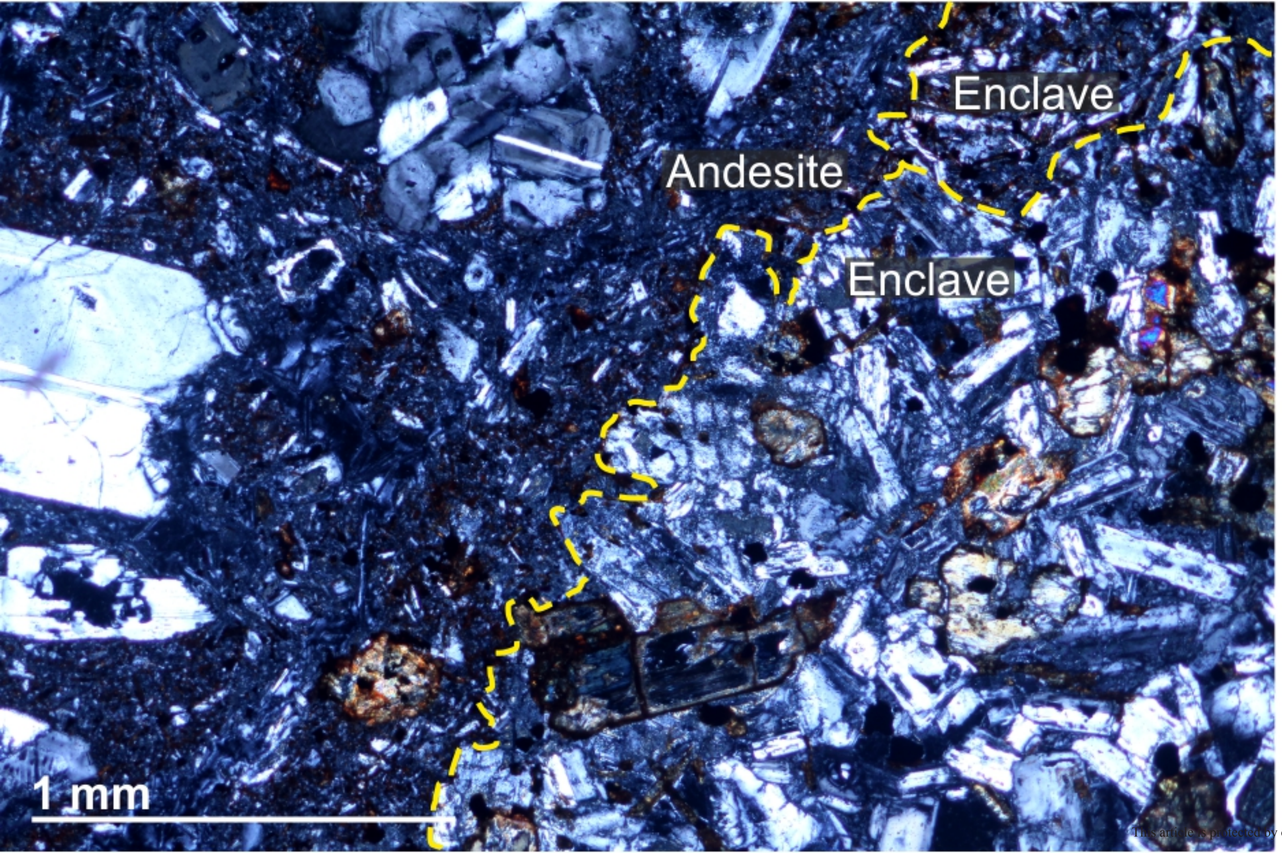

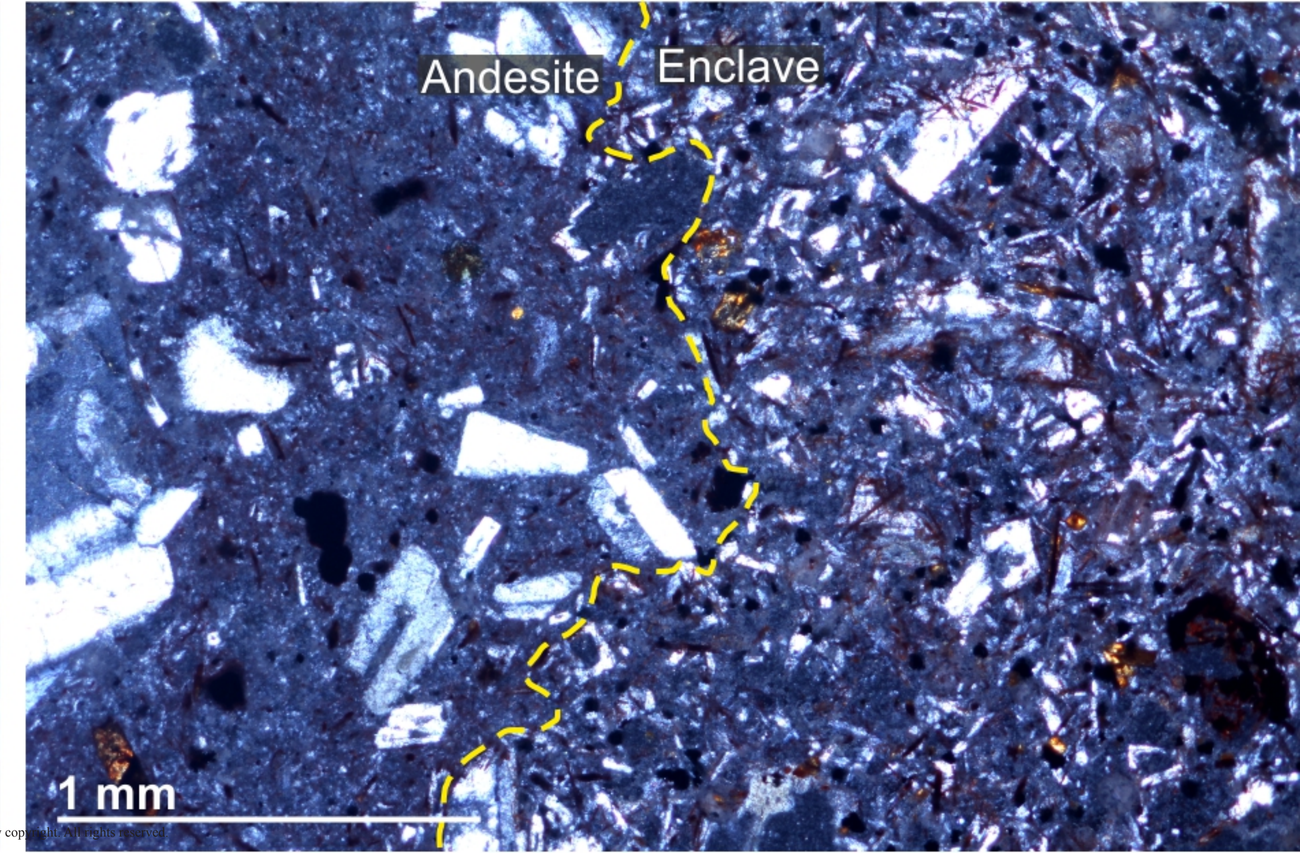

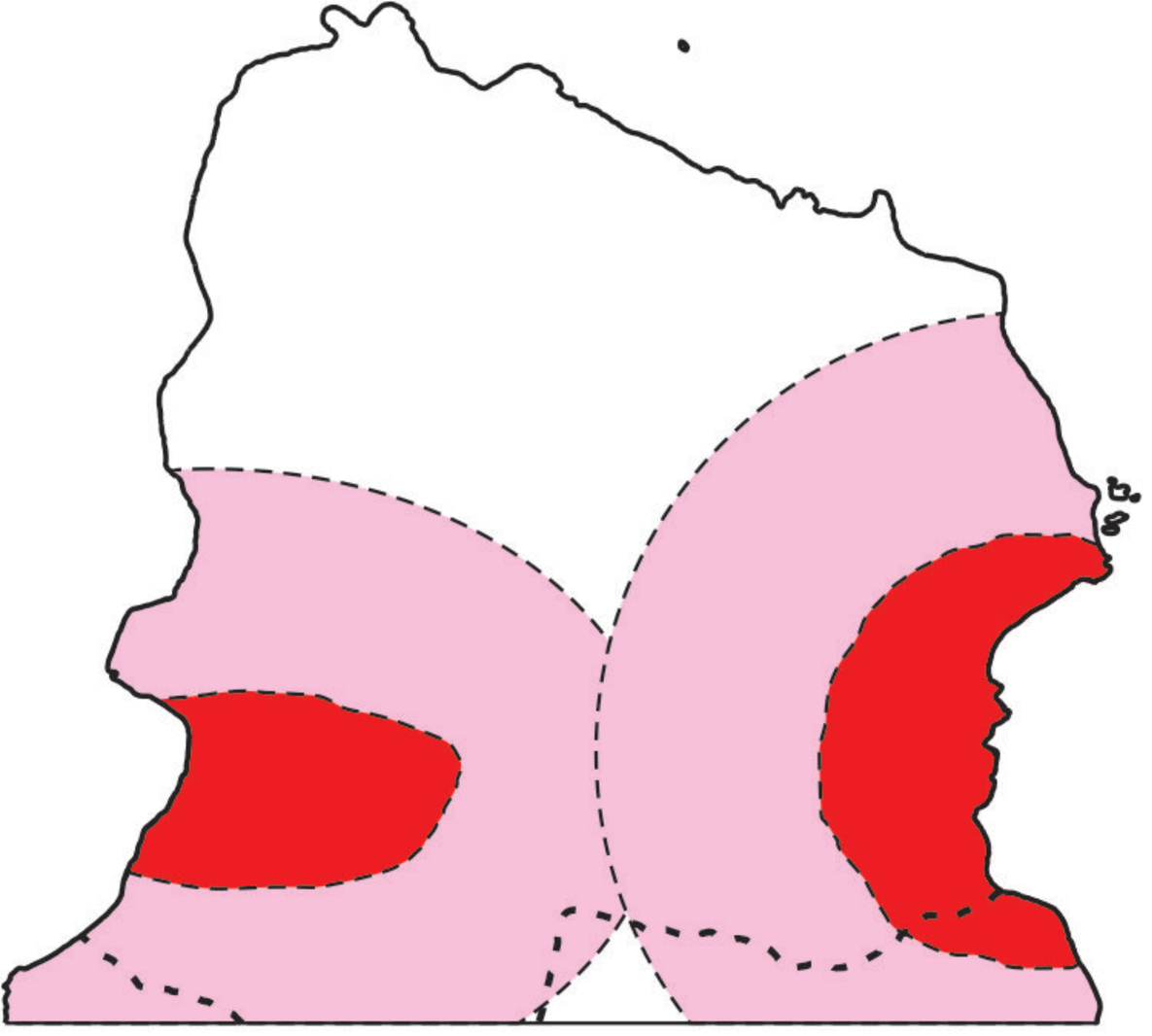

~2.17 Ma: Little Bay | 1.7–1.6 Ma: Marguerita Bay

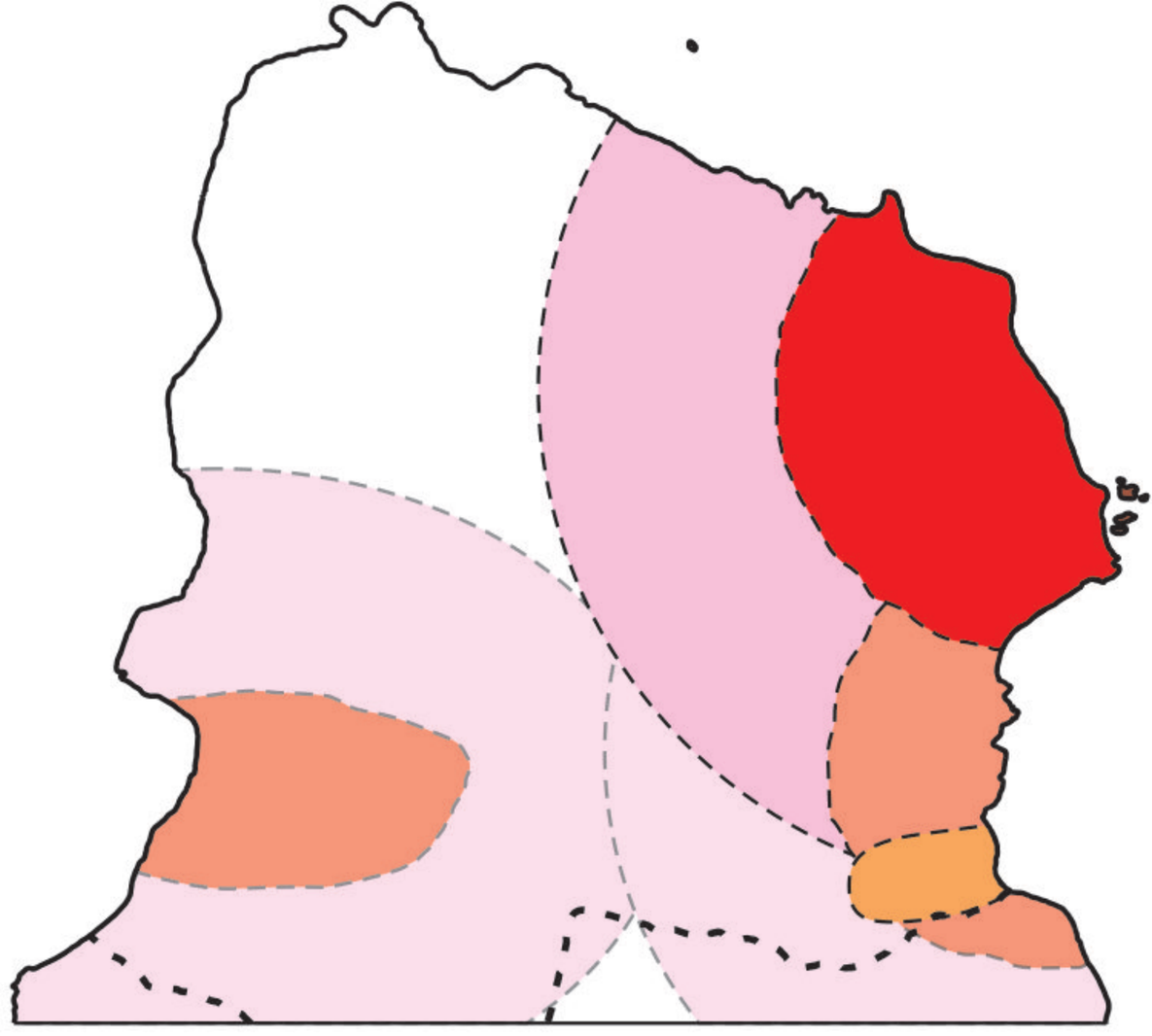

1.5 Ma: Yellow Hole

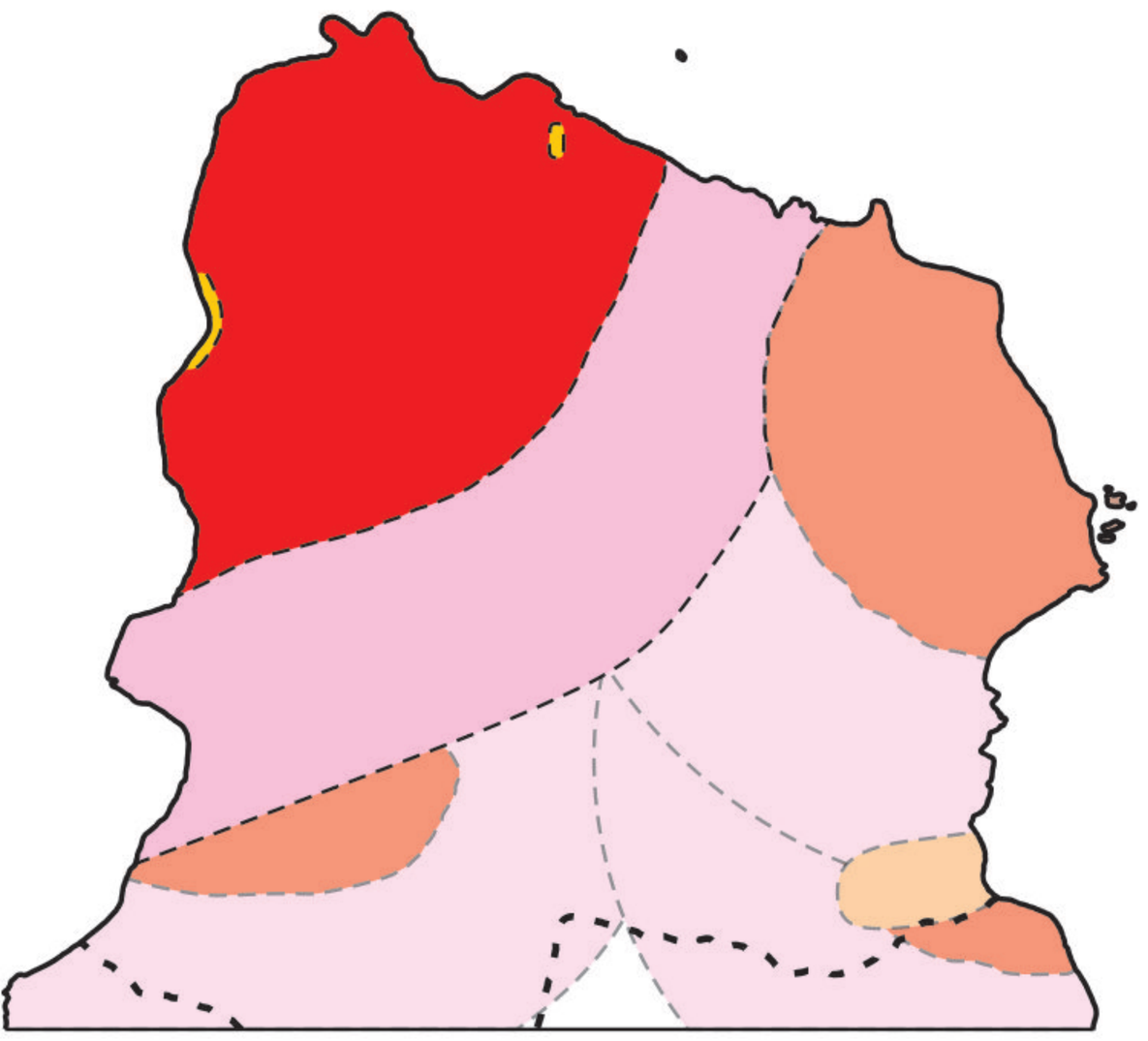

1.5–1.4 Ma: Northwest Bluff

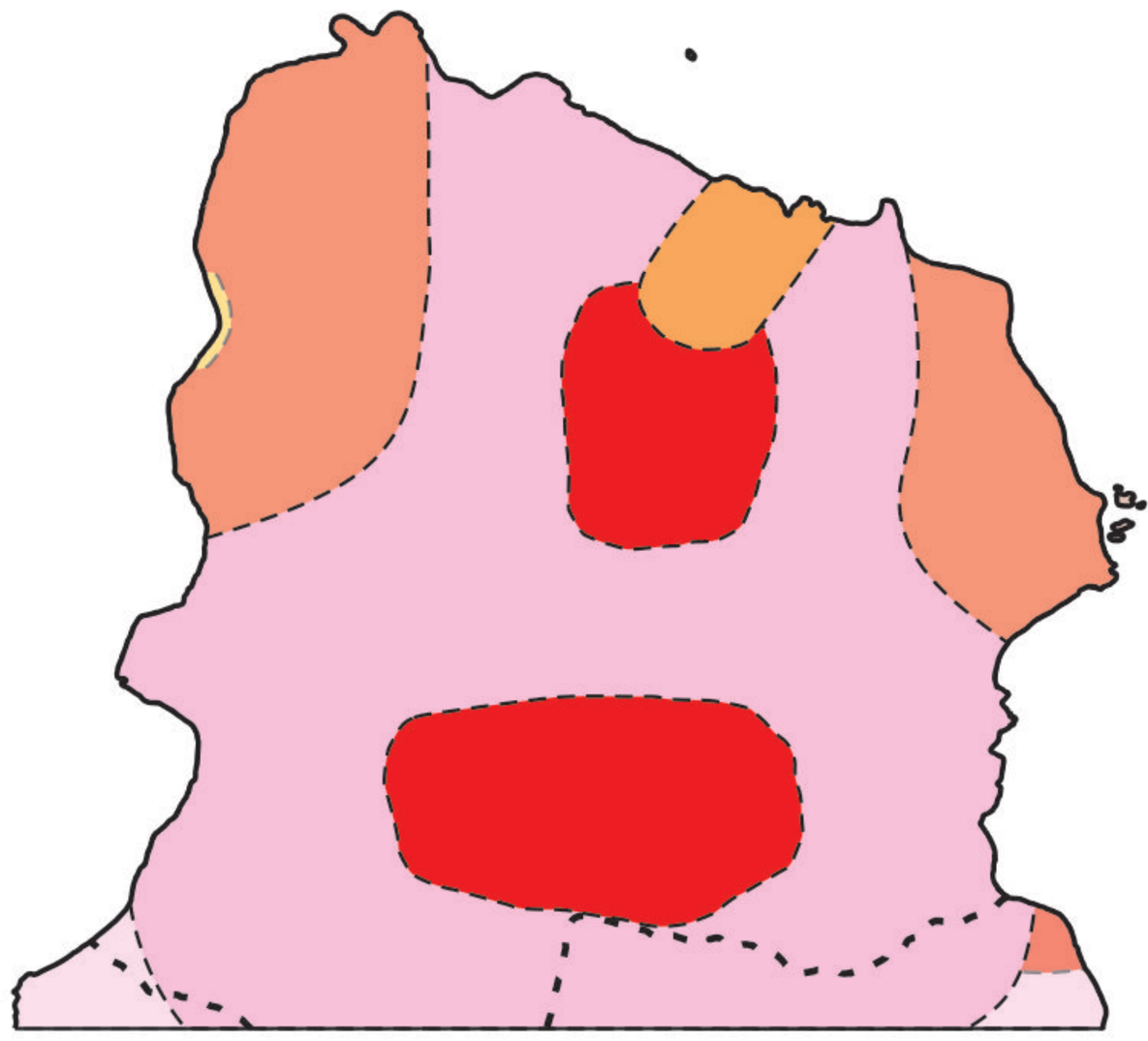

1.4 Ma: Silver Hill and Drummonds

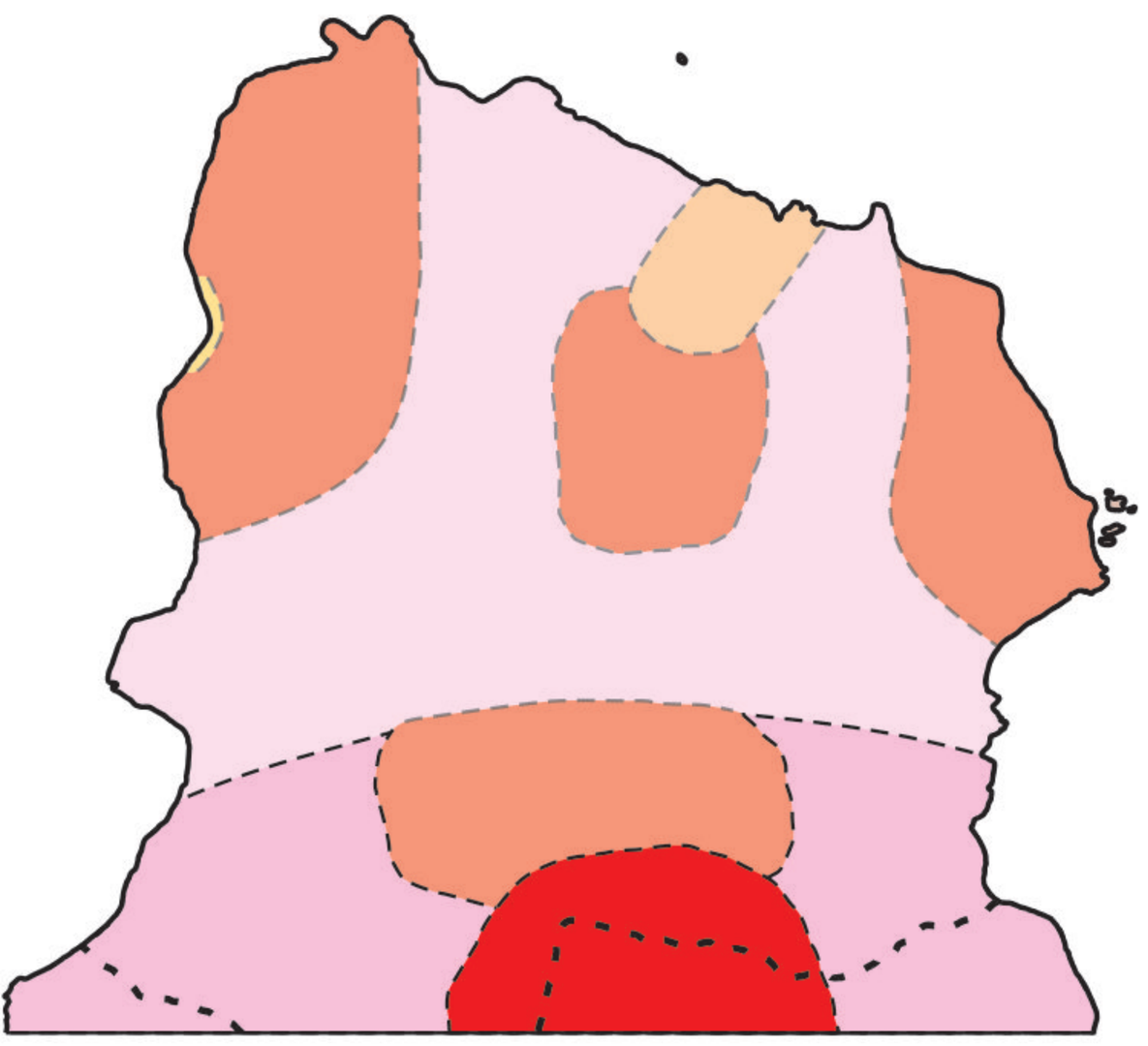

1.3 Ma: South Drummonds

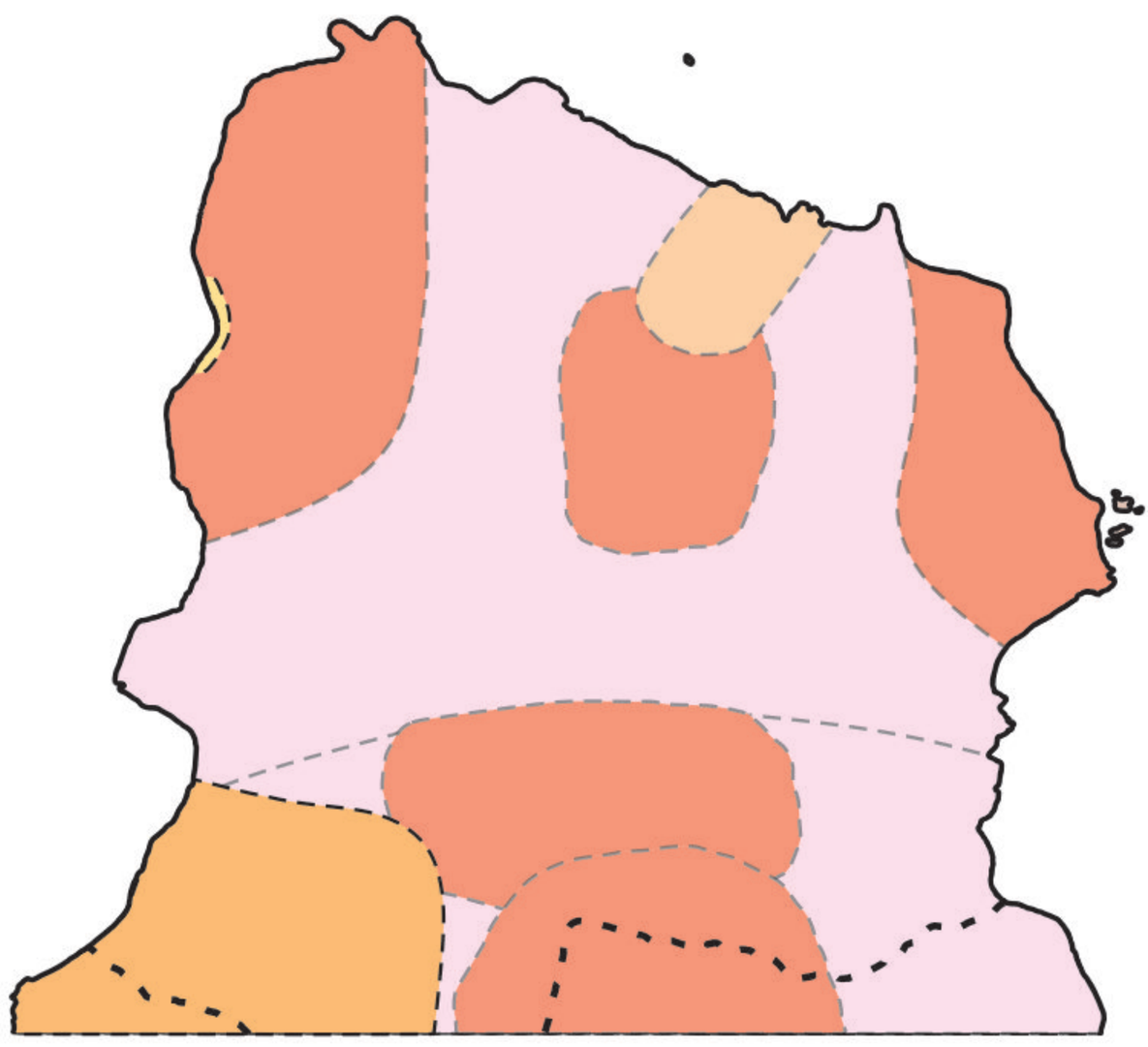

~1.0–0.8 Ma: Little Bay debris avalanche

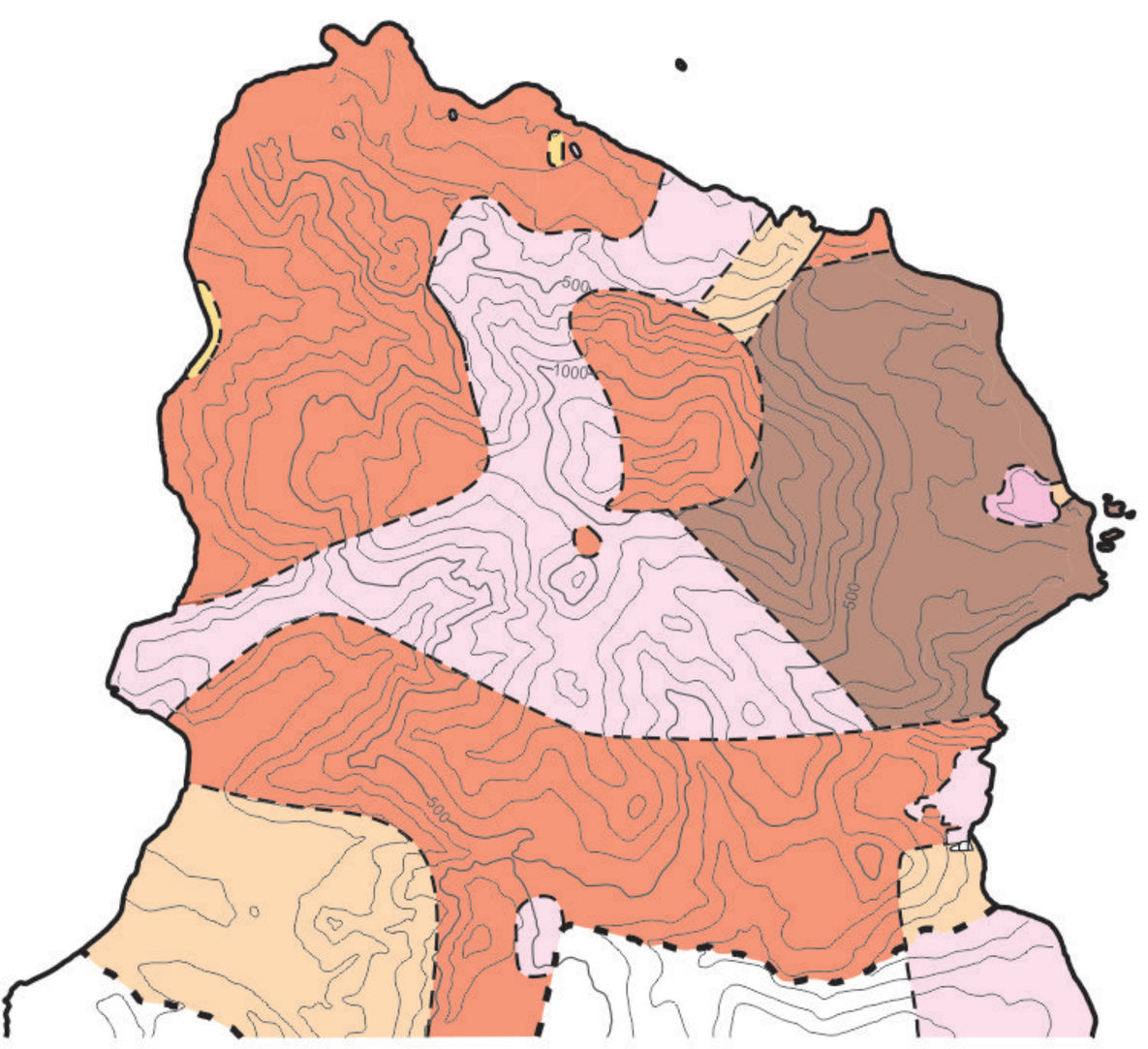

Present Day

Key

- Lava
- Block-and-ash flow deposit
- Reworked fallout deposit
- Undifferentiated debris avalanche deposit
- Fumarole deposit
- Undifferentiated lavas and breccias
- Recent landslide